Journal of Engineering Mathematics (2005) 52: 63–91
DOI 10.1007/s10665-004-7952-7

Perturbation solutions for flow through symmetrical hoppers with inserts and asymmetrical wedge hoppers

G.M. COX*, S.W. MCCUE[1], N. THAMWATTANA and J.M. HILL
School of Mathematics and Applied Statistics, University of Wollongong, Wollongong, 2522, N.S.W., Australia
**Author for correspondence (E-mail: gcox@uow.edu.au); [1]Currrent address: School of Science, Griffith University, Nathan 4111, QLD Australia*

Received 19 July 2004; accepted in revised form 20 December 2004

Abstract. Under certain circumstances, an industrial hopper which operates under the "funnel-flow" regime can be converted to the "mass-flow" regime with the addition of a flow-corrective insert. This paper is concerned with calculating granular flow patterns near the outlet of hoppers that incorporate a particular type of insert, the cone-in-cone insert. The flow is considered to be quasi-static, and governed by the Coulomb–Mohr yield condition together with the non-dilatant double-shearing theory. In two-dimensions, the hoppers are wedge-shaped, and as such the formulation for the wedge-in-wedge hopper also includes the case of asymmetrical hoppers. A perturbation approach, valid for high angles of internal friction, is used for both two-dimensional and axially symmetric flows, with analytic results possible for both leading order and correction terms. This perturbation scheme is compared with numerical solutions to the governing equations, and is shown to work very well for angles of internal friction in excess of 45°.

Key words: asymmetric hoppers, Coulomb-Mohr yield condition, granular flow, hopper inserts, perturbation solution

1. Introduction

Granular materials are used extensively throughout the world in most industrial processes, where these materials are stored in hoppers (or silos), which are large containers designed to provide easy retrieval. Disruptions to the flow of the material from a hopper often arise due to phenomena such as arching (see [1] for a thorough review) and rat-holing (see [2–4]). For both phenomena the underlying mechanisms of initiation and formation are not properly understood, and to gain a better understanding of these situations, improved models are necessary. The ability to accurately predict the flow distribution of material from a hopper is of great importance, especially when disruptions to flow reduce the productivity and profitability of the industrial process concerned. Ideally, hoppers should be designed to operate in a prescribed manner, giving reliable flow-rates, which in turn leads to an increase in both the profit and viability of the industrial process.

In general, the desired flow pattern in an industrial hopper is where the entire material in the hopper is simultaneously in motion, commonly referred to as "mass-flow". Conversely, an undesired flow pattern is where flow occurs only in a central region that is surrounded by a stagnant region, and is referred to as "funnel-flow". Parameters that contribute to whether the flow pattern is mass-flow or funnel-flow include the slope and smoothness of the walls and the cohesiveness and the inter-particle friction of the material. As such, studying the flow behaviour for varying parameters should lead to a deeper understanding of hopper flow of granular

materials, enabling improved predictions as to whether a particular hopper with a particular material will give rise to mass-flow or funnel-flow.

One of the methods of converting a funnel-flow hopper into a mass-flow hopper is to use an insert (for experimental studies, see: [5–8]; and for numerical simulations, see: [9,10]). An insert is an apparatus (usually metal), which is fastened at a fixed position in a silo or hopper, in order to influence the flow of granular material in such a way as to prohibit the formation of funnel-flow. The three most common types of inserts are "cone-in-cone", "inverted cone" and "double cone", as shown in Figure 1. Here we are primarily interested in investigating the effect of the cone-in-cone inserts [5,9,10]. As described by Dantoin et al. [11], funnel-flow hoppers can cause serious problems to industrial processes. In [11], a situation is described where due to the build-up of stagnant material in a coal funnel-flow bunker at a power plant, an explosion occurred that caused in excess of \$US 4 million in damages and loss production. Further, after the event, another \$US 1·2 millon was spent in upgrading the funnel-flow bunker to a mass-flow bunker. Accordingly, any improvement in our understanding of the flow patterns of hoppers with inserts has the potential to provide the particulate industries with a much cheaper option in regard to converting a funnel-flow hopper into a mass-flow hopper.

Gravity flow of granular material from a hopper has been studied extensively throughout the literature, with a review of some developments given in [12], and some more recent studies in [13,14], for example. Early progress for this problem was made in [15–18], where the so-called "radial stress field" solutions are studied for quasi-static flow of incompressible materials which obey the Coulomb–Mohr yield condition. These solutions are similarity solutions, and are valid in the neighbourhood of the hopper outlet. In this case the equilibrium equations and the Coulomb–Mohr yield condition reduce to two highly non-linear coupled ordinary differential equations, which in general can only be solved numerically. Recently, some exact parametric solutions to these equations have been determined by Cox and Hill [19] and Hill and Cox [20] for the limiting case of $\sin\phi = 1$, where ϕ is the angle of internal friction of the material. Furthermore, these exact solutions have been recently used by Thamwattana and Hill [21] as leading order terms in a regular perturbation valid for $1 - \sin\phi \ll 1$. There do exist granular materials that possess angles of internal friction around 60 to 65°, as supported by the experimental data given in [22, p. 23], [23–25]. Such materials give rise to values of $\sin\phi$ around 0·87 to 0·91, and we refer to materials with $1 - \sin\phi \ll 1$ as being "highly frictional". Of course, we must be cautious when studying high-friction granular materials, as the physics involved in taking the limit $\phi \to \pi/2$ is not well-understood (and could be the subject of experimental investigations). However, in the present study, as with [21], we are interested in deriving solutions for $1 - \sin\phi$ small but finite, so the question of the validity of setting $\phi = \pi/2$ is not relevant here.

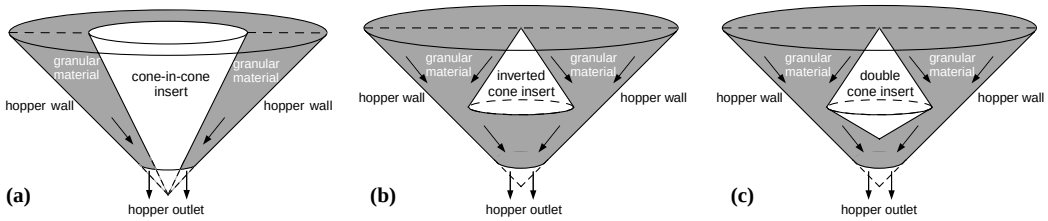

Figure 1. Schematic diagram of conical hopper with a cone-in-cone insert (a), an inverted cone insert (b), and a double-cone insert (c).

The use of the Coulomb–Mohr yield condition to predict stress fields in quasi-static granular flows is quite widely accepted, and produces results that are well in accord with experimental data. However, the correct formulation of the accompanying velocity equations is still controversial. To accompany the radial stress fields described above, [15,17] use the coaxial flow rule to describe the velocity fields. This approach assumes the principal axes of stress and strain-rate coincide. An alternate flow rule comes from the double-shearing theory, originally proposed by Spencer [26,27]. In this theory, every deformation is assumed to consist of simultaneous shears along the two families of stress lines, and (for quasi-static flow) the characteristic curves for the stresses and velocities coincide. For the flow of material near the outlet of a hopper, [28,29] show the coaxial theory used in [15,17] yields physically unacceptable predictions in the velocity field, whereas the double-shearing theory predicts results which are certainly reasonable. Further, [30] compares the double-shearing theory with experimental results for this problem, and the agreement is excellent. Exact velocity fields for the limiting case of $\phi = \pi/2$ have been calculated in [31] using the double-shearing theory. These solutions have yet to be employed as leading-order terms in a perturbation series, and this is one of the goals of the present study.

In this paper, we consider the two-dimensional problems of quasi-static granular flow through asymmetrical wedge hoppers and hoppers with wedge-in-wedge inserts, as well as the axially symmetric problem of flow through conical hoppers with cone-in-cone inserts. In the following section we formulate the governing ordinary differential equations which apply near the outlet of the hoppers, and derive the appropriate boundary conditions in each case. In Sections 3 and 4 we attack the problems by considering a regular perturbation series, following [21], by assuming that the quantity $1-\sin\phi \ll 1$, remembering that ϕ is the angle of internal friction. The first two terms of the expansion are found parametrically, and it is shown that these analytic results provide excellent approximations to the exact numerical solutions for values of ϕ in excess of 45°, particularly for steep hoppers, and the necessary physical condition of the rate of work being non-negative is examined in Section 5. Finally, in Section 6 we make some concluding remarks.

2. Mathematical formulation

In this section we briefly state the governing equations for steady quasi-static granular flow through two-dimensional and axially symmetric hoppers under gravity. In two-dimensions, boundary conditions are given for hoppers whose walls have unequal slopes, a situation which includes the case of a wedge-in-wedge insert. For axially symmetric flows, boundary conditions are given for the case in which there is a cone-in-cone insert.

2.1. Governing equations in two-dimensions

We consider here steady flow of a granular material in two dimensions, and use cylindrical polar coordinates (r,θ) as defined by Figures 2(a) and (b). By assuming the flow is quasi-static, the inertia terms in the momentum equations may be neglected, so that the components of the Cauchy stress tensor $\sigma_{rr}, \sigma_{\theta\theta}$ and $\sigma_{r\theta}$ satisfy the equilibrium equations

$$\frac{\partial\sigma_{rr}}{\partial r}+\frac{1}{r}\frac{\partial\sigma_{r\theta}}{\partial\theta}+\frac{\sigma_{rr}-\sigma_{\theta\theta}}{r}=\rho g\sin\theta, \quad \frac{\partial\sigma_{r\theta}}{\partial r}+\frac{1}{r}\frac{\partial\sigma_{\theta\theta}}{\partial\theta}+\frac{2\sigma_{r\theta}}{r}=\rho g\cos\theta, \tag{2.1}$$

where ρ is the bulk density and g is acceleration due to gravity. In this study the material is taken to be incompressible, so that the density ρ is constant. We note the stress components

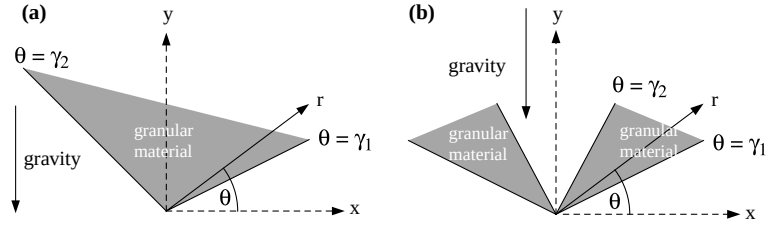

Figure 2. Coordinate system for a two-dimensional asymmetrical wedge hopper (a), and a two-dimensional hopper with a wedge-in-wedge insert (b).

are assumed to be positive in tension, so that a positive force will produce a positive extension.

To close the system of equations, we assume the material yields according to the Coulomb–Mohr yield condition. Thus, for every surface through an arbitrary point within the material, the magnitude of the tangential component of the traction vector τ_n is bounded by the critical value

$$|\tau_n| \leq c - \sigma_n \tan\phi, \tag{2.2}$$

where σ_n is the normal component of tensive traction on the surface. Here, $c \geq 0$ denotes the cohesion of the material, while $0 \leq \phi \leq \pi/2$ is the angle of internal friction, both assumed constant. We note if equality holds in (2.2), then the material yields at that point along the particular surface whose tangential and normal components of traction are given by τ_n and σ_n, respectively.

Now, to utilize the above equations, we introduce the stress angle ψ defined by

$$\tan 2\psi = \frac{2\sigma_{r\theta}}{\sigma_{rr} - \sigma_{\theta\theta}}, \tag{2.3}$$

where physically ψ corresponds to the angle between the direction corresponding to the maximum principal stress and the r-axis, in the direction of increasing θ. Next, upon introducing the generally positive stress invariants p and q defined by

$$p = -\frac{1}{2}(\sigma_I + \sigma_{III}) = -\frac{1}{2}(\sigma_{rr} + \sigma_{\theta\theta}), \quad q = \frac{1}{2}(\sigma_I - \sigma_{III}) = \frac{1}{2}\left\{(\sigma_{rr} - \sigma_{\theta\theta})^2 + 4\sigma_{r\theta}^2\right\}^{1/2}, \tag{2.4}$$

the usual stress decomposition arises

$$\sigma_{rr} = -p + q\cos 2\psi, \quad \sigma_{\theta\theta} = -p - q\cos 2\psi, \quad \sigma_{r\theta} = q\sin 2\psi, \tag{2.5}$$

where σ_I and σ_{III} denote the maximum and minimum principal stresses respectively, and physically speaking, p represents an average pressure, while q is the maximum magnitude of the shear stress. This stress decomposition enables the equilibrium equations to be expressed in terms of an equivalent formulation using p, q and ψ.

To express the Coulomb–Mohr yield condition using these three variables, we note that for an arbitrary surface whose unit normal **n** makes an angle of δ with the positive x-axis, the normal tensive component and the magnitude of the tangential component of traction are given by

$$\sigma_n = -p + q\cos 2(\delta - \psi), \quad |\tau_n| = q|\sin 2(\delta - \psi)|. \tag{2.6}$$

As the quantity $|\tau_n| + \sigma_n \tan\phi$ attains its maximum possible value when

$$\delta = \psi \pm \left(\frac{\pi}{4} - \frac{\phi}{2}\right), \tag{2.7}$$

then from (2.2), yield only occurs along surfaces whose normal **n** makes an angle of δ given by (2.7). Further, we denote the normal tensive component and the magnitude of the tangential component of traction of such surfaces by σ and τ, respectively, so that from (2.6) and (2.7) we find

$$\sigma = -p + q\sin\phi, \quad \tau = q\cos\phi. \tag{2.8}$$

As a result, for yielding material, we can express the Coulomb–Mohr yield condition in the more useful form of

$$q = p\sin\phi + c\cos\phi. \tag{2.9}$$

Now, [16, 17] show that a radial stress field solution is a reasonable approximation for the stress distribution near the outlet of a hopper. This involves a radial wedge field solution of the form

$$\psi = \psi(\theta), \quad q = \rho g r F(\theta), \tag{2.10}$$

so from (2.5) and (2.9) we find that the equilibrium Equations (2.1) give rise to two non-linear coupled ordinary differential equations, namely

$$\frac{\mathrm{d}F}{\mathrm{d}\theta} = \frac{F\sin 2\psi - \beta\cos(\theta + 2\psi)}{\beta + \cos 2\psi}, \quad 1 + \frac{\mathrm{d}\psi}{\mathrm{d}\theta} = \frac{F(\beta^{-1} - \beta) + \sin\theta + \beta\sin(\theta + 2\psi)}{2F(\beta + \cos 2\psi)}, \tag{2.11}$$

where here and throughout the paper we use the notation $\beta = \sin\phi$. We can eliminate F from the governing Equations (2.11), and deduce the single second-order ordinary differential equation for $\psi(\theta)$

$$\begin{aligned}(\beta + \cos 2\psi)[\sin\theta + \beta\sin(\theta + 2\psi)]\psi'' = 2(1 + \psi')\{\sin 2\psi[\sin\theta + \beta\sin(\theta + 2\psi)]\psi' + \\ + 2\beta\cos(\theta + 2\psi)(\beta + \cos 2\psi)\psi' + (3\beta^2 + 2\beta\cos 2\psi - 1)\cos(\theta + 2\psi)\},\end{aligned} \tag{2.12}$$

where the primes denote differentiation with respect to θ. With ψ determined, the function F can be recovered from

$$F = \frac{\beta[\sin\theta + \beta\sin(\theta + 2\psi)]}{2\beta(\beta + \cos 2\psi)(1 + \psi') + \beta^2 - 1}. \tag{2.13}$$

As mentioned in the Introduction, the above equations are generally accepted as a reasonable basis for the determination of the plane-strain stress field for gravity flow from a hopper; however, the prescription of the governing equations for the determination of the velocity field is not as readily agreed upon. In this study we assume the velocity profile is governed by the non-dilatant double-shearing theory derived by Spencer [26, 27], which is based on the idea that deformation arises as a result of shear along the surfaces defined by (2.7) on which the critical shear stress is mobilized, and which coincide with the slip-lines in quasi-static flows. In particular, if $v_r(r, \theta)$ and $v_\theta(r, \theta)$ are the components of velocity in the r and θ, directions, respectively, then the double-shearing theory provides that they satisfy the following equations

$$\begin{aligned}&\frac{\partial v_r}{\partial r} + \frac{1}{r}\frac{\partial v_\theta}{\partial \theta} + \frac{v_r}{r} = 0, \\ &\left(\frac{\partial v_\theta}{\partial r} + \frac{1}{r}\frac{\partial v_r}{\partial \theta} - \frac{v_\theta}{r}\right)\cos 2\psi - \left(\frac{\partial v_r}{\partial r} - \frac{1}{r}\frac{\partial v_\theta}{\partial \theta} - \frac{v_r}{r}\right)\sin 2\psi = \beta\left(\frac{\partial v_\theta}{\partial r} - \frac{1}{r}\frac{\partial v_r}{\partial \theta} - \frac{v_\theta}{r} - 2\Omega\right),\end{aligned} \tag{2.14}$$

where the quantity Ω is defined to be

$$\Omega = v_r \frac{\partial \psi}{\partial r} + \frac{v_\theta}{r} \frac{\partial \psi}{\partial \theta}. \tag{2.15}$$

Following [15], for hopper flow we assume the particular velocity profile

$$v_r(r, \theta) = \frac{u(\theta)}{r}, \quad v_\theta(r, \theta) = 0, \tag{2.16}$$

which ensures that flow can only occur in the radial direction, and $(2.14)_1$ is automatically satisfied. In this case, recalling that $\psi = \psi(\theta)$, then $(2.14)_2$ becomes simply

$$\frac{\mathrm{d}u}{\mathrm{d}\theta}(\beta + \cos 2\psi) = -2u \sin 2\psi, \tag{2.17}$$

which implies that

$$u = \bar{u} \exp\left\{2 \int_\theta^{\theta_c} \frac{\sin 2\psi}{\beta + \cos 2\psi} \, \mathrm{d}\theta\right\}, \tag{2.18}$$

for some constants θ_c and $\bar{u}$ such that $\bar{u} = u(\theta_c)$. We note that $\bar{u}$ is the arbitrary constant of integration arising from solving (2.17), while θ_c is a constant that has been introduced to ensure that $u/\bar{u} = 1$ at some specific angle $\theta = \theta_c$ (which is done in order to facilitate the comparison of the perturbation solution with a numerical solution). In particular, we choose $\theta_c = \pi/2$ for the asymmetrical wedge hopper, and $\theta_c = \gamma_2$ for the hopper with a wedge-in-wedge insert.

2.2. Boundary conditions for two-dimensional flow

In this subsection we specify appropriate boundary conditions for the problems of flow in an asymmetrical wedge hopper and flow in a hopper with a wedge-in-wedge insert, as shown in Figure 2(a) and (b). For the latter problem we need only consider half of the hopper, since the flow field is symmetric. The two mathematical problems are essentially the same, with the exception being the physical range of values of γ_1 and γ_2. In particular, for the asymmetrical wedge hopper we have $0 < \gamma_1 < \pi/2 < \gamma_2 < \pi$, while for the hopper with an insert we instead have $0 < \gamma_1 < \gamma_2 < \pi/2$ (with the other half of the flow given by reflection). We note that the problem of an asymmetrical wedge hopper is in some respects similar to the non-axially symmetric hopper flows considered recently in [14].

In all the problems we are considering in this study, it is assumed that the cohesion is zero ($c = 0$), and as the material flows along the sidewalls of the hopper and the sidewalls of the insert, it is reasonable that a Coulomb friction condition should apply along these walls. In this case, upon examining the geometry of the problems as depicted in Figure 2, we find that the two-dimensional Cauchy stress components must satisfy the boundary conditions

$$\sigma_{r\theta} = \sigma_{\theta\theta} \tan \mu_1 \text{ at } \theta = \gamma_1, \quad \sigma_{r\theta} = -\sigma_{\theta\theta} \tan \mu_2 \text{ at } \theta = \gamma_2, \tag{2.19}$$

where μ_1 and μ_2 denote the angles of wall friction of the sidewall of the hopper along $\theta = \gamma_1$ and $\theta = \gamma_2$, respectively. Thus, from (2.5) and (2.9) we find for a cohesionless material that the two-dimensional boundary conditions (2.19) become

$$\sin[\mu_1 + 2\psi(\gamma_1)] = -\frac{\sin \mu_1}{\sin \phi} \text{ at } \theta = \gamma_1, \quad \sin[\mu_2 - 2\psi(\gamma_2)] = -\frac{\sin \mu_2}{\sin \phi} \text{ at } \theta = \gamma_2, \tag{2.20}$$

which are valid provided $\mu_1 < \phi$ and $\mu_2 < \phi$. If the material is such that $\mu_1 \geq \phi$ or $\mu_2 \geq \phi$, then the material will slip on itself at the wall, and here the wall is referred to as being "perfectly rough". We do not consider this case in the present study. We note that if we assume

the cohesion is non-zero, then the Coulomb friction conditions cannot be satisfied (unless $\phi = \pi/2$), as detailed in [32].

In summary, the problem of computing the stress and velocity fields near the outlet of a two-dimensional asymmetrical wedge hopper reduces to solving the non-linear ordinary differential equation (2.12) subject to the boundary conditions (2.20), with $F(\theta)$ and $u(\theta)$ then given by (2.13) and (2.18), respectively. In general, this can only be achieved by solving (2.12) numerically, with a finite-element scheme, for example. However for large values of the angle of internal friction ϕ we seek analytic progress in Section 3 using perturbation analysis.

2.3. Governing equations with axial symmetry

For axially symmetric flows through conical hoppers it is appropriate to use spherical coordinates (R, Θ, Φ), as defined by Figure 3. In this case the four independent components of the stress tensor, denoted by $\sigma_{RR}, \sigma_{\Theta\Theta}, \sigma_{\Phi\Phi}$ and $\sigma_{R\Theta}$, are independent of the variable Φ. We will employ the usual stress decomposition

$$\sigma_{RR} = -P + Q\cos 2\Psi, \quad \sigma_{\Theta\Theta} = -P - Q\cos 2\Psi, \quad \sigma_{R\Theta} = Q\sin 2\Psi, \tag{2.21}$$

where P and Q are the stress invariants given by

$$P = -\frac{1}{2}(\sigma_I + \sigma_{III}) = -\frac{1}{2}(\sigma_{RR} + \sigma_{\Theta\Theta}), \quad Q = \frac{1}{2}(\sigma_I - \sigma_{III}) = \frac{1}{2}\left\{(\sigma_{RR} - \sigma_{\Theta\Theta})^2 + 4\sigma_{R\Theta}^2\right\}^{1/2}, \tag{2.22}$$

with σ_I and σ_{III} denoting the maximum and minimum principal stresses, respectively. Further, Ψ is the stress angle defined by

$$\tan 2\Psi = \frac{2\sigma_{R\Theta}}{\sigma_{RR} - \sigma_{\Theta\Theta}}, \tag{2.23}$$

where physically Ψ corresponds to the angle between the direction corresponding to the maximum principal stress and the R-axis, in the direction of increasing Θ.

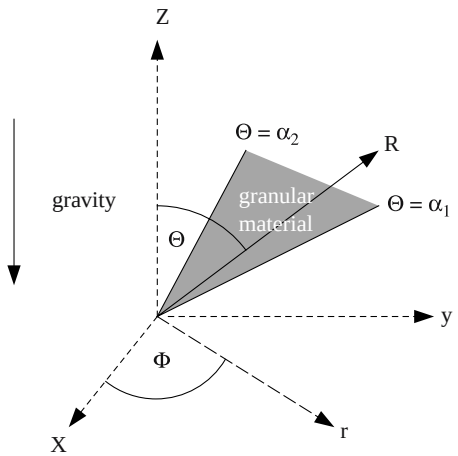

Figure 3. Coordinate system for a three-dimensional hopper with a cone-in-cone insert.

For quasi-static flow, the stress components satisfy the equilibrium equations

$$\begin{aligned}
&\frac{\partial \sigma_{RR}}{\partial R}+\frac{1}{R}\frac{\partial \sigma_{R\Theta}}{\partial \Theta}+\frac{2\sigma_{RR}-\sigma_{\Theta\Theta}-\sigma_{\Phi\Phi}}{R}+\frac{\sigma_{R\Theta}}{R}\cot\Theta=\rho g\cos\Theta,\\
&\frac{\partial \sigma_{R\Theta}}{\partial R}+\frac{1}{R}\frac{\partial \sigma_{\Theta\Theta}}{\partial \Theta}+\frac{\sigma_{\Theta\Theta}-\sigma_{\Phi\Phi}}{R}\cot\Theta+\frac{3\sigma_{R\Theta}}{R}=-\rho g\sin\Theta,
\end{aligned} \tag{2.24}$$

which can be rewritten in terms P, Q, Ψ and $\sigma_{\Phi\Phi}$, but we leave out the details here. In addition, we have the Coulomb–Mohr yield condition (2.2), which is written in terms of P and Q as

$$Q=P\sin\phi+c\cos\phi. \tag{2.25}$$

We therefore have three Equations (2.24) and (2.25) to describe the stress field, with the four unknowns P, Q, Ψ (or σ_{RR}, $\sigma_{\Theta\Theta}$, $\sigma_{R\Theta}$) and $\sigma_{\Phi\Phi}$.

To close the system of equations we need to make an assumption about the hoop stress, in order to determine an expression for $\sigma_{\Phi\Phi}$ in terms of P, Q and Ψ. It has been stated in [33] that the plastic regimes which agree with the Haar-von Kármán hypothesis will give rise to solutions that are most likely to be of the greatest significance to axially symmetric problems of interest. In particular, the heuristic Haar-von Kármán principle states that under an axially symmetric condition the hoop stress is equal to either the maximum or minimum principal stress. This condition gives rise to the idea of Haar-von Kármán regimes, and in particular, either $\sigma_I=\sigma_{\Phi\Phi}=\sigma_{II}>\sigma_{III}$ or $\sigma_I>\sigma_{II}=\sigma_{\Phi\Phi}=\sigma_{III}$, where σ_{II} denotes the intermediate principal stress, and in both cases the hoop stress $\sigma_{\Phi\Phi}$ is assumed to be a principal stress. Here, we choose the former, from which we may deduce

$$\sigma_{\Phi\Phi}=-P+Q. \tag{2.26}$$

We note that this choice differs from the traditional view (see [15,16,28]), in which more physically realistic results for the converging conical hopper problem are believed to be produced by choosing $\sigma_{\Phi\Phi}=\sigma_{III}$, leading to

$$\sigma_{\Phi\Phi}=-P-Q, \tag{2.27}$$

while (2.26) is believed as being more applicable for diverging flow. However, with (2.27) we have been unable to determine an exact parametric solution for the limiting case of $\phi=\pi/2$, and as such, analytic progress with a perturbation scheme for $1-\sin\phi\ll 1$ has not been possible. We therefore adopt (2.26) and we keep in mind that the results obtained may not be as physically applicable as those obtained when $\sigma_{\Phi\Phi}$ is given by (2.27).

Now, following [15–17], we assume a stress field solution of the form

$$\Psi=\Psi(\Theta),\quad Q=\rho g R G(\Theta), \tag{2.28}$$

so from (2.21), (2.25) and (2.26) we find that the equilibrium Equations (2.24) give rise to two non-linear coupled ordinary equations, namely

$$\begin{aligned}
&\frac{\mathrm{d}G}{\mathrm{d}\theta}=\frac{2G\cos\Psi\{\sin\Psi-\beta\,\mathrm{cosec}\Theta\cos(\Theta+\Psi)\}+\beta\sin(\Theta+2\Psi)}{\beta+\cos 2\Psi},\\
&1+\frac{\mathrm{d}\Psi}{\mathrm{d}\Theta}=\frac{G(1-\beta)\{\beta^{-1}(1+2\beta)-\mathrm{cosec}\Theta\sin(\Theta+2\Psi)\}+\cos\Theta+\beta\cos(\Theta+2\Psi)}{2G(\beta+\cos 2\Psi)},
\end{aligned} \tag{2.29}$$

where again we adopt the notation $\beta=\sin\phi$. We can eliminate G from the governing Equations (2.29), and deduce the single second-order ordinary differential equation for $\Psi(\Theta)$

$$
\begin{aligned}
&2(\beta+\cos 2\Psi)[\cos\Theta+\beta\cos(\Theta+2\Psi)]\Psi''\\
&\quad=2(1+\Psi')\Big\{\operatorname{cosec}\Theta\Big[\beta(\beta+\cos 2\Psi)[1+\cos\{2(\Theta+\Psi)\}]-\\
&\qquad-[\cos\Theta+\beta\cos(\Theta+2\Psi)][2\sin\Theta\sin 2\Psi+(1-\beta)\cos(\Theta+2\Psi)]+\\
&\qquad+2(1-\beta)\sin(\Theta+2\Psi)[(1+2\beta)\sin\Theta-\beta\sin(\Theta+2\Psi)]\Big]+\\
&\qquad+2(1+\Psi')\Big[\sin 2\Psi[\cos\Theta+\beta\cos(\Theta+2\Psi)]-2\beta\sin(\Theta+2\Psi)(\beta+\cos 2\Psi)\Big]\Big\}+\\
&\qquad+(1-\beta)\operatorname{cosec}^2\Theta\Big\{\sin\{2(\Theta+\Psi)\}[\cos\Theta+\beta\cos(\Theta+2\Psi)]-\\
&\qquad-[1+\cos\{2(\Theta+\Psi)\}][(1+2\beta)\sin\Theta-\beta\sin(\Theta+2\Psi)]\Big\},
\end{aligned}
\tag{2.30}
$$

where prime denotes differentiation with respect to Θ. With Ψ determined, the function G can be recovered from

$$
G=\frac{\beta[\cos\Theta+\beta\cos(\Theta+2\Psi)]}{2\beta(\beta+\cos 2\Psi)(1+\Psi')-(1-\beta)[1+2\beta-\beta\operatorname{cosec}\Theta\sin(\Theta+2\Psi)]}. \tag{2.31}
$$

We note the choice of the Haar-von Kármán regime (2.27) leads to a system of coupled non-linear ordinary differential equations analogous to (2.29), where the only differences involve sign changes (see [19] for full details). For this case, [34] identify a simple exact solution that provides an envelope for solutions in (Ψ, Θ) space for the problem of converging flow through a conical hopper without an insert. This envelope can be very useful, as it provides a bound for the hopper angle. If the hopper angle is larger than that given by the envelope curve, then the material must be in funnel-flow. Unfortunately, for the choice of (2.26), the corresponding exact solution (see Equation (2.29) in [19]) does not take real values, and hence cannot be used as an envelope curve. We therefore do not have a simple criterion for mass-flow when adopting (2.26).

Now, upon assuming the velocity profile is governed by the non-dilatant double-shearing theory, and if $V_R(R,\Theta)$ and $V_\Theta(R,\Theta)$ are the components of velocity in the R and Θ directions respectively, we obtain

$$
\begin{aligned}
&\frac{\partial V_R}{\partial R}+\frac{1}{R}\frac{\partial V_\Theta}{\partial\Theta}+\frac{2V_R}{R}+\frac{V_\Theta}{R}\cot\Theta=0,\\
&\left(\frac{\partial V_\Theta}{\partial R}+\frac{1}{R}\frac{\partial V_R}{\partial\Theta}-\frac{V_\Theta}{R}\right)\cos 2\Psi-\left(\frac{\partial V_R}{\partial R}-\frac{1}{R}\frac{\partial V_\Theta}{\partial\Theta}-\frac{V_R}{R}\right)\sin 2\Psi=\beta\left(\frac{\partial V_\Theta}{\partial R}-\frac{1}{R}\frac{\partial V_R}{\partial\Theta}-\frac{V_\Theta}{R}-2\Omega\right),
\end{aligned}
\tag{2.32}
$$

where the quantity Ω is defined to be

$$
\Omega=V_R\frac{\partial\Psi}{\partial R}+\frac{V_\Theta}{R}\frac{\partial\Psi}{\partial\Theta}. \tag{2.33}
$$

Following [15], we assume the velocity profile

$$
V_R(R,\Theta)=\frac{U(\Theta)}{R^2},\ V_\Theta(R,\Theta)=0, \tag{2.34}
$$

which ensures that flow can only occur in the radial direction and $(2.32)_1$ is automatically satisfied. In this case, recalling that $\Psi=\Psi(\Theta)$, then $(2.32)_2$ becomes simply

$$
\frac{\mathrm{d}U}{\mathrm{d}\Theta}(\beta+\cos 2\Psi)=-3U\sin 2\Psi, \tag{2.35}
$$

which implies that

$$
U=\bar{U}\exp\left\{-3\int_{\Theta_c}^{\Theta}\frac{\sin 2\Psi}{\beta+\cos 2\Psi}\,\mathrm{d}\Theta\right\}, \tag{2.36}
$$

for some constants Θ_c and $\bar{U}$ such that $\bar{U} = U(\Theta_c)$. We note that $\bar{U}$ is the arbitrary constant of integration arising from solving (2.35), while Θ_c is a known constant that has been introduced to ensure that $U/\bar{U} = 1$ at some specific angle $\Theta = \Theta_c$. In particular, we choose $\Theta_c = \alpha_2$ for the hopper with a cone-in-cone insert.

2.4. Boundary conditions for axially symmetric flow

In this subsection we specify appropriate boundary conditions for the problem of flow in a hopper with a cone-in-cone insert, as shown in Figure 3. We note that the physical range of values of α_1 and α_2 must satisfy $0 < \alpha_2 < \alpha_1 < \pi/2$.

As with the two-dimensional problem, we assume that the cohesion is zero ($c = 0$), and that a Coulomb friction condition applies along the hopper walls. It follows from the problem geometry (see Figure 3) that the axially symmetric Cauchy stress components must satisfy

$$\sigma_{R\Theta} = -\sigma_{\Theta\Theta} \tan \mu_1 \text{ at } \Theta = \alpha_1, \quad \sigma_{R\Theta} = \sigma_{\Theta\Theta} \tan \mu_2 \text{ at } \Theta = \alpha_2, \tag{2.37}$$

where μ_1 and μ_2 denote the angles of wall friction of the sidewall of the hopper along $\Theta = \alpha_1$ and $\Theta = \alpha_2$, respectively. Thus, from (2.21) and (2.25) we find for a cohesionless material that the axially symmetric boundary conditions (2.37) become

$$\sin[\mu_1 - 2\Psi(\alpha_1)] = -\frac{\sin \mu_1}{\sin \phi} \text{ at } \Theta = \alpha_1, \quad \sin[\mu_2 + 2\Psi(\alpha_2)] = -\frac{\sin \mu_2}{\sin \phi} \text{ at } \Theta = \alpha_2, \tag{2.38}$$

which are valid provided $\mu_1 < \phi$ and $\mu_2 < \phi$. As with the two-dimensional case, we mention that, if either $\mu_1 \geq \phi$ or $\mu_2 \geq \phi$, then the material will slip on itself at the appropriate wall, the wall being referred to as "perfectly rough". Since we are primarily concerned with materials with high angles of internal friction, we do not consider this case here.

In summary, the problem for computing the stress and velocity fields near the outlet of an axially symmetric hopper with a cone-in-cone insert reduces to solving the non-linear ordinary differential equation (2.30) subject to the boundary conditions (2.38), with $G(\Theta)$ and $U(\Theta)$ then given by (2.31) and (2.36), respectively. In general, this can only be achieved by solving (2.30) numerically, however, in Section 4 we derive analytic solutions via a perturbation scheme valid when the quantity $1 - \sin \phi \ll 1$.

3. Highly frictional limit in two-dimensions

In this section we seek analytic solutions to the two-dimensional problems formulated in Section 2 by considering the asymptotic limit $\phi \to \pi/2$. For $\phi = \pi/2$ there has been a great deal of success recently in deriving exact solutions for gravity-driven quasi-static flow (see [35], for example), and for the particular case of the similarity solutions described by (2.10) and (2.16), these solutions have been used as leading-order terms in perturbation series for $1 - \sin \phi \ll 1$ in [21]. Here we extend this analysis to hold for asymmetrical wedge hoppers and hoppers with wedge-in-wedge inserts.

3.1. Perturbation analysis

We analyse the governing Equations (2.12), (2.13) and (2.18) by writing out the solutions in the form

$$\psi = \psi_0(\theta) + \epsilon \psi_1(\theta) + O(\epsilon^2), \quad F = F_0(\theta) + \epsilon F_1(\theta) + O(\epsilon^2), \quad u = u_0(\theta) + \epsilon u_1(\theta) + O(\epsilon^2), \tag{3.1}$$

where $\epsilon = 1-\beta = 1-\sin\phi$ and $\epsilon \ll 1$. To leading order we find that ψ_0 satisfies the non-linear ordinary differential equation

$$\psi_0'' = 2(1+\psi_0')\left\{\cot(\theta+\psi_0)(1+\psi_0') - \tan\psi_0\right\}, \tag{3.2}$$

and F_0 and u_0 are given in terms of ψ_0 by

$$F_0 = \frac{\sin(\theta+\psi_0)}{2(1+\psi_0')\cos\psi_0},\ u_0 = \bar{u}\exp\left\{2\int_\theta^{\theta_c}\tan\psi_0\,\mathrm{d}\theta\right\}. \tag{3.3}$$

The leading-order terms ψ_0, F_0 and u_0 are evidently the solutions for the ideal limit $\phi = \pi/2$. These equations were first solved by Hill and Cox [20], and the solution procedure is briefly described here. We make the transformation

$$h(\xi) = \cot(\theta+\psi_0), \quad \xi = \tan\theta, \tag{3.4}$$

and (3.2) becomes

$$(h+\xi)h'' + 2h' = 0, \tag{3.5}$$

where the primes here indicate derivatives with respect to ξ. This equation can be solved by introducing the substitutions $\nu(\xi) = h+\xi$, $\omega(\nu) = 1-\nu'(\xi)$, for some intermediate variable ν, the result being that the solution is given parametrically by

$$h = \cot(\theta+\psi_0) = \frac{I(\omega)}{C_2}, \quad \xi = \tan\theta = \frac{2\omega^{-1/2}\mathrm{e}^{\omega/2} - I(\omega)}{C_2}, \tag{3.6}$$

where ω acts as a parameter, $I(\omega)$ is the integral defined by

$$I(\omega) = \int_0^\omega t^{-1/2}\mathrm{e}^{t/2}\mathrm{d}t + C_1, \tag{3.7}$$

and C_1 and C_2 are arbitrary constants. It follows that the solutions for F_0 and u_0 are given parametrically by

$$F_0 = \frac{1}{4}\frac{\omega^{-1/2}\mathrm{e}^{-\omega/2}[C_2^2 + I^2(\omega)]}{\left\{C_2^2 + [2\omega^{-1/2}\mathrm{e}^{\omega/2} - I(\omega)]^2\right\}^{1/2}}, \quad u_0 = \frac{\bar{u}\,\omega\left\{C_2^2 + [2\omega^{-1/2}\mathrm{e}^{\omega/2} - I(\omega)]^2\right\}}{\omega_c\left\{C_2^2 + [2\omega_c^{-1/2}\mathrm{e}^{\omega_c/2} - I(\omega_c)]^2\right\}}, \tag{3.8}$$

where the parameter value $\omega = \omega_c$ corresponds to $\theta = \theta_c$.

The correction term for the stress angle ψ_1 is found to satisfy the linear equation

$$\begin{aligned}\psi_1'' = {} & 2\psi_1'\left\{2(\psi_0'+1)\cot(\theta+\psi_0) - \tan\psi_0\right\} + \psi_1\{\psi_0''[3\tan\psi_0 - \cot(\theta+\psi_0)] - \\ & -2(\psi_0'+1)^2[1+3\tan\psi_0\cot(\theta+\psi_0)] + 2(\psi_0'+1)[2\tan^2\psi_0 - \tan\psi_0\cot(\theta+\psi_0) - 1]\} + \\ & +(\psi_0'+1)^2[\tan\psi_0\mathrm{cosec}^2(\theta+\psi_0) + \sec^2\psi_0(\tan\psi_0 - \cot(\theta+\psi_0)] - (\psi_0'+1)\sec^2\psi_0\cot(\theta+\psi_0),\end{aligned} \tag{3.9}$$

where ψ_0 is given by the leading-order solution (3.6). The method for solving this ordinary differential equation is presented in Appendix A, along with the analysis for determining F_1 and u_1. The result is that the correction terms are given by

$$\psi_1 = \frac{1}{C_2^2 + I^2(\omega)} \left\{ C_4(1-\omega) + \tfrac{1}{4}[2\omega^{1/2}\mathrm{e}^{\omega/2} + (1-\omega)I(\omega)] \left[\int_0^\omega (1-t)K(t)\mathrm{d}t + C_3 \right] - \right.$$
$$\left. -\tfrac{1}{4}(1-\omega) \int_0^\omega [2t^{1/2}\mathrm{e}^{t/2} + (1-t)I(t)]K(t)\mathrm{d}t \right\},$$
$$F_1 = F_0 \frac{\omega^{1/2}\mathrm{e}^{-\omega/2}}{8C_2^2}[C_2^2 + I^2(\omega)] \left\{ 8C_2 \frac{\mathrm{d}\psi_1}{\mathrm{d}\omega} + 4C_2\psi_1 + (1+\omega)\omega^{-1/2}\mathrm{e}^{-\omega/2}[C_2^2 + I^2(\omega)] - \right. \quad (3.10)$$
$$\left. -6I(\omega) + \frac{8\omega^{-1/2}\mathrm{e}^{\omega/2}I^2(\omega)}{C_2^2 + I^2(\omega)} \right\},$$
$$u_1 = \frac{u_0}{8C_2^2} \left\{ \mathrm{e}^{-\omega_c}[C_2^2 + I^2(\omega_c)]^2 - \mathrm{e}^{-\omega}[C_2^2 + I^2(\omega)]^2 \right.$$
$$\left. +2 \int_{\omega_c}^\omega t^{-1/2}\mathrm{e}^{-t/2}[C_2^2 + I^2(t)][2C_2\psi_1 + I(t)]\mathrm{d}t \right\},$$

where C_3 and C_4 are constants of integration, F_0 given by $(3.8)_1$, u_0 given by $(3.8)_2$, and the function K given by the expression

$$K(\omega) = -\frac{1}{2C_2}\omega^{-1/2}\mathrm{e}^{-\omega/2}I(\omega)[C_2^2 + I^2(\omega)] - \frac{2}{C_2}\omega^{-1/2}\mathrm{e}^{\omega/2}[2\omega^{-1/2}\mathrm{e}^{\omega/2} - I(\omega)] +$$
$$+\frac{1}{4C_2}\omega\mathrm{e}^{-\omega}[C_2^2 + (2\omega^{-1/2}\mathrm{e}^{\omega/2} - I(\omega))^2]^2. \quad (3.11)$$

3.2. Application of boundary conditions

By substituting the perturbation series $(3.1)_1$ in the boundary conditions (2.20), we find that

$$\psi_0 = -\mu_1, \quad \psi_1 = -\tfrac{1}{2}\tan\mu_1 \quad \text{on} \quad \theta = \gamma_1,$$
$$\psi_0 = \mu_2, \quad \psi_1 = \tfrac{1}{2}\tan\mu_2 \quad \text{on} \quad \theta = \gamma_2. \quad (3.12)$$

In this subsection we use these conditions to determine the values of the constants C_1 and C_2 in the leading-order solution ψ_0 given by (3.6)–(3.7), and the constants C_3 and C_4 in the correction term ψ_1 in $(3.10)_1$. Throughout this section we will use the integral

$$J(\omega) = \int_0^\omega t^{-1/2}\mathrm{e}^{t/2}\ \mathrm{d}t, \quad (3.13)$$

so that from (3.7) we have $I(\omega) = J(\omega) + C_1$.

3.2.1. *Wedge-in-wedge insert*

For the case of a wedge-in-wedge insert (see Figure 2) we need only consider the domain $\gamma_1 \leq \theta \leq \gamma_2$, since the flow is symmetric about $\theta = \pi/2$. We suppose that the parameter ω in (3.6) takes the values $\omega = \omega_1$ and $\omega = \omega_2$ at $\theta = \gamma_1$ and $\theta = \gamma_2$, respectively. By applying the boundary conditions $(3.12)_1$ and $(3.12)_3$, we find the constants C_1 and C_2 are given in terms of these parameter values by

$$C_1 = C_2\cot(\gamma_2 + \mu_2) - J(\omega_2),\ C_2 = \frac{2\omega_1^{-1/2}\mathrm{e}^{\omega_1/2} - J(\omega_1) + J(\omega_2)}{\tan\gamma_1 + \cot(\gamma_2 + \mu_2)},$$

while the values of ω_1 and ω_2 are determined by the pair of transcendental equations

$$\tfrac{1}{2}\omega_1^{1/2}\mathrm{e}^{-\omega_1/2}[J(\omega_1)-J(\omega_2)]=\frac{\cot(\gamma_1-\mu_1)-\cot(\gamma_2+\mu_2)}{\tan\gamma_1+\cot(\gamma_1-\mu_1)},$$

$$\left(\frac{\omega_2}{\omega_1}\right)^{1/2}\mathrm{e}^{(\omega_1-\omega_2)/2}=\frac{\tan\gamma_1+\cot(\gamma_1-\mu_1)}{\tan\gamma_2+\cot(\gamma_2+\mu_2)}.$$

The other two boundary conditions $(3.12)_2$ and $(3.12)_4$ provide the following equations for C_3 and C_4

$$C_3=\frac{1}{mM(\omega_2)-M(\omega_1)}\left\{2(m\tan\mu_2[C_2^2+I^2(\omega_2)]+\tan\mu_1[C_2^2+I^2(\omega_1)])+\right.$$
$$\left.+(1-\omega_1)\int_{\omega_1}^{\omega_2}M(t)K(t)\mathrm{d}t-mM(\omega_2)\int_0^{\omega_2}(1-t)K(t)\mathrm{d}t+M(\omega_1)\int_0^{\omega_1}(1-t)K(t)\mathrm{d}t\right\},$$
$$C_4=\frac{1}{mM(\omega_2)-M(\omega_1)}\left\{-\frac{1}{2(1-\omega_2)}(\tan\mu_1M(\omega_2)[C_2^2+I^2(\omega_1)]+\tan\mu_2M(\omega_1)[C_2^2+I^2(\omega_2)])-\right.$$
$$\left.-\frac{M(\omega_1)M(\omega_2)}{4(1-\omega_2)}\int_{\omega_2}^{\omega_1}(1-t)K(t)\mathrm{d}t+\frac{1}{4}\left[mM(\omega_2)\int_0^{\omega_1}M(t)K(t)\mathrm{d}t-M(\omega_1)\int_0^{\omega_2}M(t)K(t)\mathrm{d}t\right]\right\},$$

where $M(\omega)$ and m are defined by

$$M(\omega)=2\omega^{1/2}\mathrm{e}^{\omega/2}+(1-\omega)I(\omega),\qquad m=\frac{1-\omega_1}{1-\omega_2},$$

respectively.

3.2.2. *Asymmetrical wedge hopper*

For the case of an asymmetrical wedge hopper, the application of the boundary conditions is not as straightforward. Here we must split up the domain into two parts, namely $\gamma_1\le\theta\le\pi/2$ and $\pi/2\le\theta\le\gamma_2$, and treat each region separately. The solutions in each part are then matched by ensuring that the stress angle ψ and its first derivative ψ' are continuous at $\theta=\pi/2$.

For the first region, $\gamma_1\le\theta\le\pi/2$, we suppose the relevant solutions are given by (3.6)–$(3.8)_2$ and $(3.10)_1$–(3.11), with $\omega=0$ corresponding to $\theta=\pi/2$ and $\omega=\omega_1$ corresponding to $\theta=\gamma_1$. In this case, from (3.6) and $(3.12)_1$, we find

$$C_2\tan\gamma_1=2\omega_1^{-1/2}\mathrm{e}^{\omega_1/2}-J(\omega_1)-C_1,\qquad C_2\cot(\gamma_1-\mu_1)=J(\omega_1)+C_1,\tag{3.14}$$

which upon solving for C_1 and C_2, gives

$$C_1=\frac{2\omega_1^{-1/2}\mathrm{e}^{\omega_1/2}\cot(\gamma_1-\mu_1)}{\tan\gamma_1+\cot(\gamma_1-\mu_1)}-J(\omega_1),\qquad C_2=\frac{2\omega_1^{-1/2}\mathrm{e}^{\omega_1/2}}{\tan\gamma_1+\cot(\gamma_1-\mu_1)}.\tag{3.15}$$

The other condition on $\theta=\gamma_1$ $(3.12)_2$ provides the equation

$$-\tfrac{1}{2}\tan\mu_1[C_2^2+I^2(\omega_1)]=C_4(1-\omega_1)-\tfrac{1}{4}(1-\omega_1)\int_0^{\omega_1}[2t^{1/2}\mathrm{e}^{t/2}+(1-t)I(t)]K(t)\mathrm{d}t$$
$$+\tfrac{1}{4}[2\omega_1^{1/2}\mathrm{e}^{\omega_1/2}+(1-\omega_1)I(\omega_1)]\left[\int_0^{\omega_1}(1-t)K(t)\mathrm{d}t+C_3\right],\tag{3.16}$$

which we will come back to.

For the other region in the hopper $\pi/2\le\theta\le\gamma_2$, we suppose that the general solutions are also given by (3.6)–$(3.8)_2$ and $(3.10)_1$–(3.11), except now we assign different labels to the

parameter and the constants of integration. Instead of the parameter ω we shall use s, and instead of the constants C_1, C_2, C_3, C_4 we shall use D_1, D_2, D_3, D_4, respectively. So for $\pi/2 \leq \theta \leq \gamma_2$ by $I(s)$ we mean $J(s) + D_1$, where $J(s)$ is defined in (3.13). For reference, these solutions are listed by Equations (B.1)–(B.4) in Appendix B. Note that in this region the parameter s takes the value $s = 0$ at $\theta = \pi/2$. We denote the value at $\theta = \gamma_2$ to be $s = s_2$. From (B.1) and $(3.12)_3$, we find

$$D_2 \tan\gamma_2 = 2s_2^{-1/2} e^{s_2/2} - J(s_2) - D_1, \quad D_2 \cot(\gamma_2 + \mu_2) = J(s_2) + D_1, \tag{3.17}$$

which upon solving for D_1 and D_2, gives

$$D_1 = \frac{2s_2^{-1/2} e^{s_2/2} \cot(\gamma_2 + \mu_2)}{\tan\gamma_2 + \cot(\gamma_2 + \mu_2)} - J(s_2), \; D_2 = \frac{2s_2^{-1/2} e^{s_2/2}}{\tan\gamma_2 + \cot(\gamma_2 + \mu_2)}. \tag{3.18}$$

Thus, once ω_1 and s_2 are known, (3.15) and (3.18) constitute four expressions for the arbitrary constants C_1, C_2, D_1 and D_2. The condition $(3.12)_4$ on $\theta = \gamma_2$ becomes

$$\begin{aligned} \tfrac{1}{2}\tan\mu_2[D_2^2 + I^2(s_2)] = D_4(1 - s_2) - \tfrac{1}{4}(1 - s_2)\int_0^{s_2} [2t^{1/2}e^{t/2} + (1-t)I(t)]K(t)\mathrm{d}t + \\ + \tfrac{1}{4}[2s_2^{1/2}e^{s_2/2} + (1 - s_2)I(s_2)]\left[\int_0^{s_2}(1-t)K(t)\mathrm{d}t + D_3\right]. \end{aligned} \tag{3.19}$$

Next, we need to ensure that $\psi(\theta)$ and $\psi'(\theta)$ remain continuous throughout the entire domain. Clearly, these quantities are continuous within the two regions $\gamma_1 \leq \theta < \pi/2$ and $\pi/2 < \theta \leq \gamma_2$, and as such, we need only examine the boundary between the two the solutions at $\theta = \pi/2$. From (3.6) and (B.1), we find at $\theta = \pi/2$ ($\omega = s = 0$) that

$$\cot[\pi/2 + \psi_0(\pi/2)] = \frac{C_1}{C_2} = \frac{D_1}{D_2}, \tag{3.20}$$

so it must be that

$$C_1 = \frac{C_2 D_1}{D_2}. \tag{3.21}$$

Further, we want $\mathrm{d}\psi_0/\mathrm{d}\theta$ to also be continuous at $\theta = \pi/2$. To do this, we first note that

$$\frac{\mathrm{d}\psi_0}{\mathrm{d}\theta} + 1 = \frac{4e^{\omega} + C_2^2\omega - 4\omega^{1/2}e^{\omega/2}(J(\omega) + C_1) + \omega(J(\omega) + C_1)^2}{C_2^2 \mathrm{cosec}^2(\theta_0 + \psi_0)}, \quad \gamma_1 \leq \theta \leq \pi/2,$$

$$\frac{\mathrm{d}\psi_0}{\mathrm{d}\theta} + 1 = \frac{4e^{s} + D_2^2 s - 4s^{1/2}e^{s/2}(J(s) + D_1) + s(J(s) + D_1)^2}{D_2^2 \mathrm{cosec}^2(\theta + \psi_0)}, \quad \pi/2 \leq \theta \leq \gamma_2,$$

so that at $\theta = \pi/2$ ($\omega = s = 0$) we find

$$\left.\frac{\mathrm{d}\psi_0}{\mathrm{d}\theta}\right|_{\theta=\pi/2} + 1 = \frac{4}{C_2^2 \mathrm{cosec}^2[\pi/2 + \psi_0(\pi/2)]} = \frac{4}{D_2^2 \mathrm{cosec}^2[\pi/2 + \psi_0(\pi/2)]}. \tag{3.22}$$

Clearly, for $\mathrm{d}\psi_0/\mathrm{d}\theta$ to be continuous, from (3.22) we require $C_2^2 = D_2^2$, so that

$$C_2 = -D_2, \tag{3.23}$$

and consequently, from (3.21) we find

$$C_1 = -D_1. \tag{3.24}$$

Similarly, by taking the limits $\omega \to 0$ and $s \to 0$ in $(3.10)_1$ and $(B.3)_1$ we find

$$\psi_1(\pi/2) = \frac{4C_4 + C_1C_3}{4(C_1^2 + C_2^2)} = \frac{4D_4 + D_1D_3}{4(D_1^2 + D_2^2)},$$

$$\left.\frac{\mathrm{d}\psi_1}{\mathrm{d}\theta}\right|_{\theta=\pi/2} = -\frac{2(C_3 - 4C_1C_4 - C_3C_1^2)}{C_2(C_1^2 + C_2^2)} = -\frac{2(D_3 - 4D_1D_4 - D_3D_1^2)}{D_2(D_1^2 + D_2^2)},$$

so that by making use of (3.23) and (3.24), we have

$$C_3 = -D_3, \quad C_4 = D_4. \tag{3.25}$$

Hence, from $(3.15)_2$, $(3.18)_2$ and (3.23), we get

$$\omega_1^{-1/2}\mathrm{e}^{\omega_1/2} = -\left[\frac{\tan\gamma_1 + \cot(\gamma_1 - \mu_1)}{\tan\gamma_2 + \cot(\gamma_2 + \mu_2)}\right] s_2^{-1/2}\mathrm{e}^{s_2/2}, \tag{3.26}$$

and from $(3.15)_1$, $(3.18)_1$ and (3.24), we obtain

$$J(\omega_1) + J(s_2) = 2\left[\frac{\cot(\gamma_2 + \mu_2) - \cot(\gamma_1 - \mu_1)}{\tan\gamma_2 + \cot(\gamma_2 + \mu_2)}\right] s_2^{-1/2}\mathrm{e}^{s_2/2}, \tag{3.27}$$

and as such, (3.26) and (3.27) constitute as two transcendental equations for ω_1 and s_2. Furthermore, together with (3.25), the conditions (3.16) and (3.19) provide simultaneous equations for C_3, C_4, D_3, D_4.

3.3. Results

In this subsection, we compare the analytic results obtained from the perturbation scheme (3.1) with the numerical results for the problem of two-dimensional flow from a hopper with a wedge-in-wedge insert, as depicted in Figure 2(b). In what follows, we choose $\gamma_1 = \pi/3$ and $\gamma_2 = 5\pi/12$, noting from [5] that the angle $\pi/2 - \gamma_1$ is generally chosen to be twice the angle $\pi/2 - \gamma_2$. Furthermore, we assume the typical values $\mu_1 = \mu_2 = \pi/12$, so that both the insert and the hopper are assumed to be made of the same material.

Figures 4, 5 and 6 show, respectively, plots of ψ, F and $u/\bar{u}$ versus the angle $\pi/2 - \theta$ for the four values of the angle of internal friction $\phi = 7\pi/18$, $\pi/3$, $\pi/4$ and $\pi/6$. In each case the solid curves correspond to the leading-order terms (3.6) and (3.8) (which are also the solutions for the limiting case $\phi = \pi/2$), while the dotted curves correspond to the first two terms in the perturbation expansion (3.1), with the correction terms given by (3.10). Finally, the dashed curves denote the full numerical solution of the governing Equations (2.12), (2.13) and (2.17). Here, the numerical solution to the second-order ordinary differential Equation (2.12) is solved using a non-linear finite-difference scheme, as described in [36, page 601], while u is found by applying a fourth-order Runge–Kutta scheme, as given is [36, page 259]. From Figure 6 we see that the material is flowing the fastest near the middle of the material, while it slows down towards both the insert and the hopper walls, due to the material being "held up" on the walls. Further, we note that due to gravity the material is moving faster at the insert wall than the hopper wall.

From these three figures, it is clear that the perturbation scheme performs extremely well for high angles of internal friction such as $\phi = 7\pi/18$ and $\phi = \pi/3$, which is to be expected. However, somewhat surprisingly, the scheme still provides an excellent approximation for the moderately high value $\phi = \pi/4$, and even provides a reasonable estimate for $\phi = \pi/6$, which is by no means a high angle of internal friction. We comment that qualitatively similar results

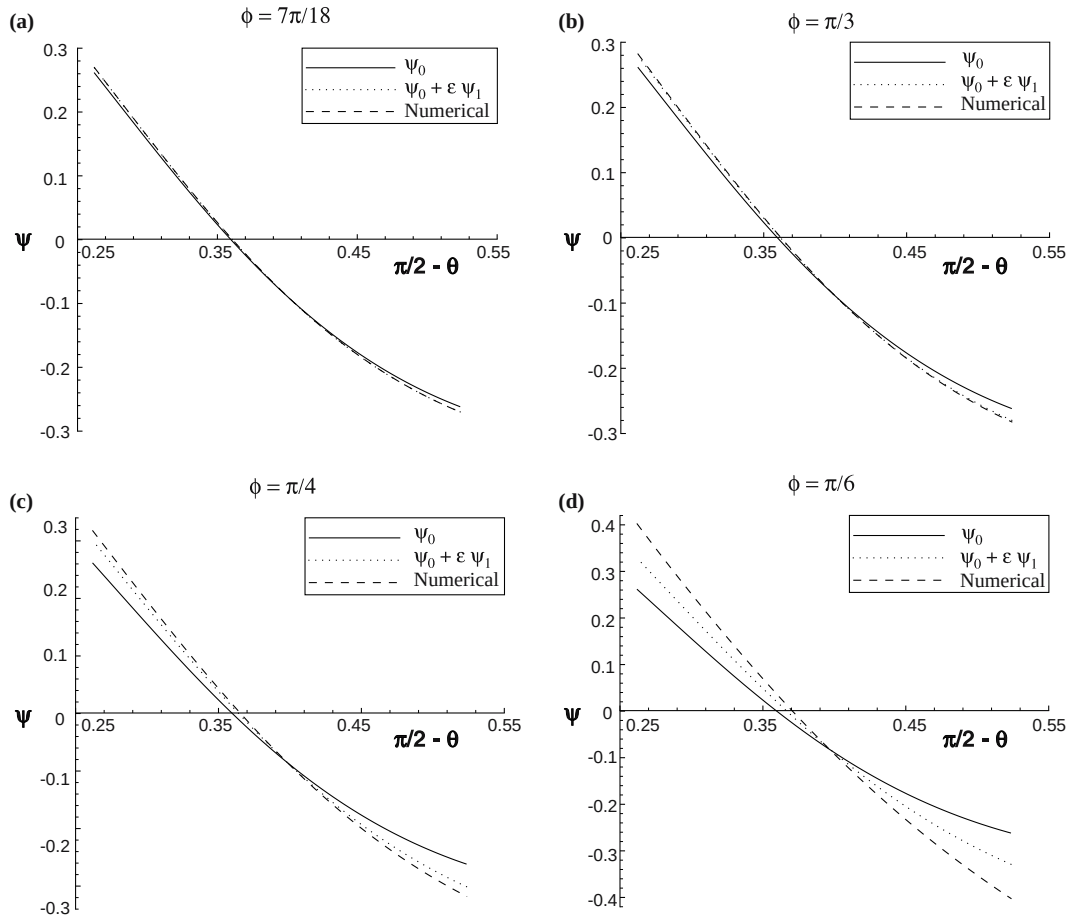

Figure 4. Comparison of the numerical, the zeroth-order and the full perturbation solutions for $\psi(\pi/2-\theta)$ for $\phi = 7\pi/18,\ \pi/3,\ \pi/4$ and $\pi/6$.

are found for different sets of α_1, α_2, μ_1 and μ_2, with the general trend being that the perturbation scheme works better for steeper hoppers.

For the sake of brevity we do not provide figures for the two-dimensional asymmetrical wedge hopper. The results are, not surprisingly, qualitatively similar to those found for the symmetric hopper, and we refer the reader to [21].

4. Highly frictional limit with axial symmetry

This section is dedicated to analysing the axially symmetric problem formulated in Sections 2.3 and 2.4 under the asymptotic limit $\phi \to \pi/2$. It is the analog of Section 3. We extend the analysis of Thamwattana and Hill [21] to hold for hoppers with cone-in-cone inserts, and we also determine the associated velocity profile according to the non-dilatant double-shearing theory.

4.1. Perturbation analysis

We seek solutions to (2.30), (2.31) and (2.36) of the form

$$\Psi = \Psi_0(\Theta) + \epsilon\Psi_1(\Theta) + O(\epsilon^2),\ G = G_0(\Theta) + \epsilon G_1(\Theta) + O(\epsilon^2),\ U = U_0(\Theta) + \epsilon U_1(\Theta) + O(\epsilon^2), \tag{4.1}$$

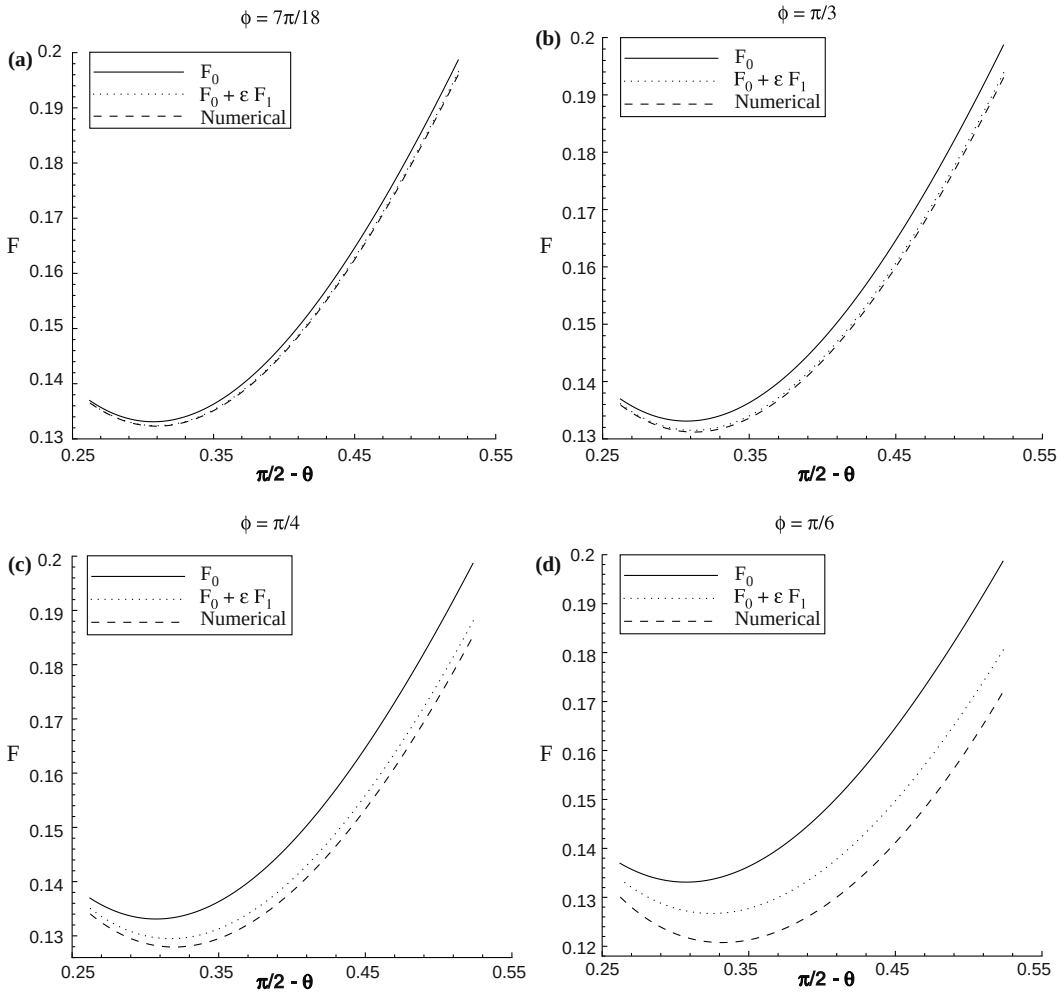

Figure 5. Comparison of the numerical, the zeroth-order and the full perturbation solutions for $F(\pi/2-\theta)$ for $\phi=7\pi/18,\ \pi/3,\ \pi/4$ and $\pi/6$.

where $\epsilon=1-\beta=1-\sin\phi$ and $\epsilon\ll 1$. To leading order, Ψ_0 satisfies the equation

$$\Psi_0''=(1+\Psi_0')\{\cot\Theta-3\tan\Psi_0-2(1+\Psi_0')\tan(\Theta+\Psi_0)\}, \tag{4.2}$$

while G_0 and U_0 are given by

$$G_0=\frac{\cos(\Theta+\Psi_0)}{2(1+\Psi_0')\cos\Psi_0},\qquad U_0=\bar{U}\exp\left\{-3\int_{\Theta_c}^{\Theta}\tan\Psi_0\mathrm{d}\Theta\right\}. \tag{4.3}$$

The leading-order terms Ψ_0, F_0 and U_0 represent solutions for the ideal limit $\phi=\pi/2$, with (4.2) and (4.3) first solved by Cox and Hill [19]. The solution procedure is analogous to that described earlier for (3.2) and (3.3), and produces the parametric result

$$H=\tan(\Theta+\Psi_0)=\frac{I(\omega)}{C_2},\ \xi=\cot\Theta=\frac{3\omega^{-1/3}\mathrm{e}^{\omega/3}-I(\omega)}{C_2}, \tag{4.4}$$

where ω is the parameter, $I(\omega)$ the integral defined by

$$I(\omega)=\int_0^{\omega}t^{-1/3}\mathrm{e}^{t/3}\ \mathrm{d}t+C_1, \tag{4.5}$$

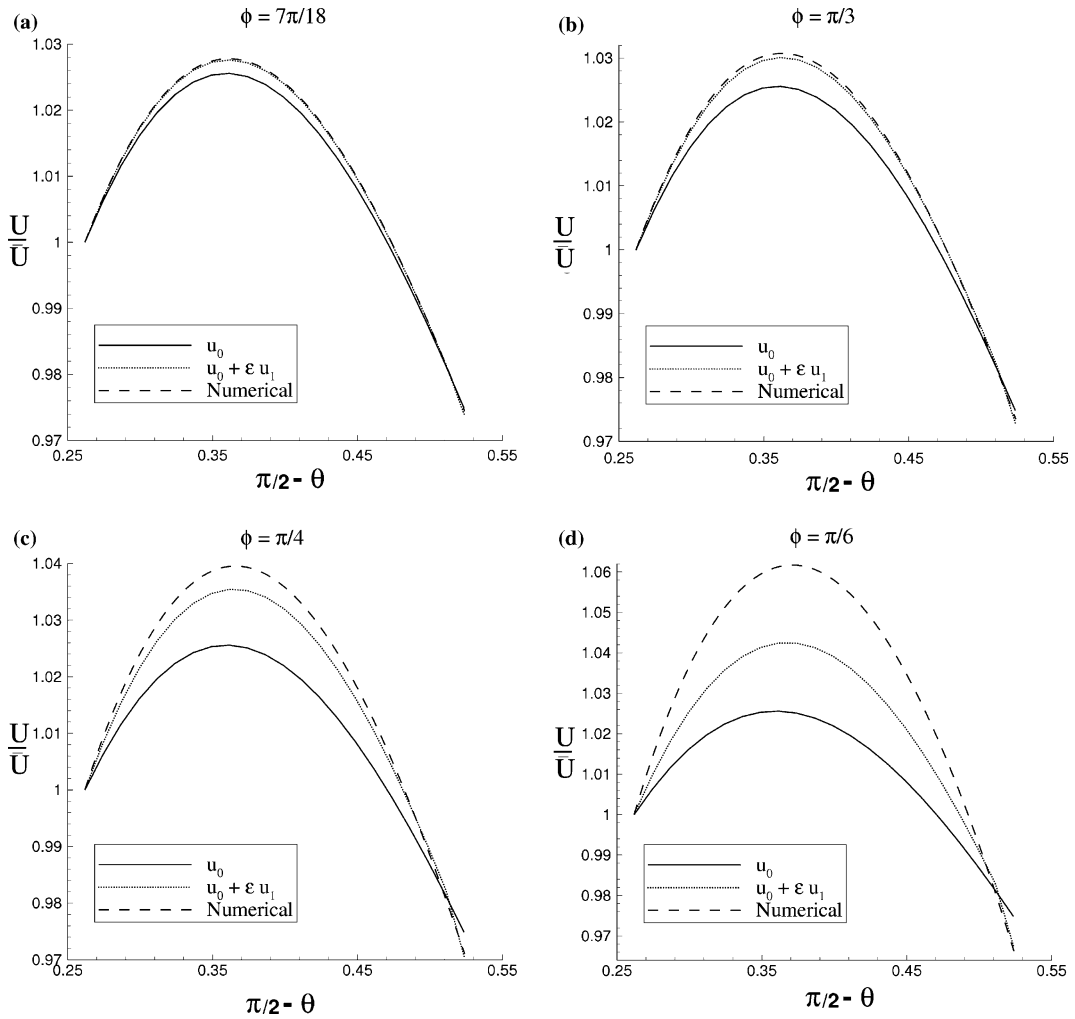

Figure 6. Comparison of the numerical, the zeroth-order and the full perturbation solutions for $u(\pi/2-\theta)/\bar{u}$ for $\phi=7\pi/18,\ \pi/3,\ \pi/4$ and $\pi/6$.

and C_1 and C_2 constants of integration. Furthermore, G_0 and U_0 are given parametrically by

$$G_0=\frac{1}{6}\frac{\omega^{-2/3}\mathrm{e}^{-\omega/3}[C_2^2+I^2(\omega)]}{\{C_2^2+[3\omega^{-1/3}\mathrm{e}^{\omega/3}-I(\omega)]^2\}^{1/2}},\qquad U_0=\frac{\bar{U}\omega\{C_2^2+[3\omega^{-1/3}\mathrm{e}^{\omega/3}-I(\omega)]^2\}^{3/2}}{\omega_c\{C_2^2+[3\omega_c^{-1/3}\mathrm{e}^{\omega_c/3}-I(\omega_c)]^2\}^{3/2}},\tag{4.6}$$

where the parameter value $\omega=\omega_c$ corresponds to $\Theta=\Theta_c$.

The correction term for the stress angle Ψ_1 is found to satisfy the linear equation

$$\begin{aligned}2\Psi_1''=&2\Psi_1'\{-4(1+\Psi_0')\tan(\Theta+\Psi_0)+\cot\theta-3\tan\Psi_0\}+2\Psi_1\{\Psi_0''[\tan(\Theta+\Psi_0)+3\tan\Psi_0]\\&2(1+\Psi_0')[(1+\Psi_0')(3\cos\Theta\sec\Psi_0\sec(\Theta+\Psi_0)-4)+\tan(\Theta+\Psi_0)(2\tan\Psi_0-\cot\Theta)+\\&+3\tan^2\Psi_0^2-\cot\Theta\tan\Psi_0-1]\}+\Psi_0''[2-\tan\Psi_0\tan(\Theta+\Psi_0)+\tan^2\Psi_0]+\\&+2(1+\Psi_0')^2[\tan(\Theta+\Psi_0)(3+2\tan^2\Psi_0)+\tan\Psi_0(2+\tan^2\Psi_0)]+\\&+(1+\Psi_0')[-2(2+\tan^2\Psi_0)(\cot\Theta-\tan\Psi_0)-(\tan\Psi_0+\tan(\Theta+\Psi_0))(1+\cot\Theta\tan\Psi_0)+\\&+\tan\Psi_0(5+3\tan^2\Psi_0)+\tan(\Theta+\Psi_0)(3+\tan^2\Psi_0)]+2\tan\Psi_0(\cot\Theta-\tan\Psi_0)^2,\end{aligned}\tag{4.7}$$

where Ψ_0 is given by the leading-order solution (4.4). The method for solving this ordinary differential equation is presented in Appendix C, along with the analysis for determining G_1 and U_1. The result is that the correction terms are given by

$$\Psi_1 = \frac{1}{C_2^2 + I^2(\omega)} \left\{ C_4(1-\omega) + \frac{1}{9}[3\omega^{2/3}\mathrm{e}^{\omega/3} + (1-\omega)I(\omega)] \left[\int_0^\omega (1-t)K(t)\mathrm{d}t + C_3 \right] \right.$$
$$\left. -\frac{1}{9}(1-\omega)\int_0^\omega [3t^{2/3}\mathrm{e}^{t/3} + (1-t)I(t)]K(t)\mathrm{d}t \right\},$$
$$G_1 = -\frac{\omega^{-1/3}\mathrm{e}^{-2\omega/3}G_0}{18C_2^2} \left\{ 18C_2\omega^{2/3}\mathrm{e}^{\omega/3}[C_2^2 + I^2(\omega)] \left(\frac{\mathrm{d}\Psi_1}{\mathrm{d}\omega} + \frac{\Psi_1}{3} \right) - [C_2^2 + I^2(\omega)]^2 \right.$$
$$\left. -[3\omega^{-1/3}\mathrm{e}^{\omega/3}I(\omega) - C_2^2 - I^2(\omega)][6\omega^{2/3}\mathrm{e}^{\omega/3}I(\omega) - (1+\omega)[C_2^2 + I^2(\omega)]] \right\},$$
$$U_1 = -\frac{U_0}{6C_2^2}\int_{\omega_c}^\omega t^{-2/3}\mathrm{e}^{-t/3}[C_2^2 + I^2(t)][2C_2\Psi_1 + I(t)]\mathrm{d}t$$
$$+\frac{U_0}{18C_2^2}\int_{\omega_c}^\omega t^{-1/3}\mathrm{e}^{-2t/3}[C_2^2 + I^2(t)]^2\mathrm{d}t, \tag{4.8}$$

where C_3 and C_4 are constants of integration, G_0 given by $(4.6)_1$, U_0 given by $(4.6)_2$, and the function K given by the expression

$$K(\omega) = \frac{C_2}{\omega} + \frac{[2I(\omega) - 3\omega^{-1/3}\mathrm{e}^{\omega/3}]^2}{C_2\omega} + \frac{3}{C_2}\omega^{-1/3}\mathrm{e}^{\omega/3}[3\omega^{-1/3}\mathrm{e}^{\omega/3} - I(\omega)] +$$
$$+\frac{1}{9C_2}\omega^{-4/3}\mathrm{e}^{-2\omega/3}[C_2^2 + I^2(\omega)][3\omega^{-1/3}\mathrm{e}^{\omega/3}I(\omega) - C_2^2 - I^2(\omega)] -$$
$$-\frac{1}{9C_2}\omega^{-1/3}\mathrm{e}^{-2\omega/3}(1+\omega)[C_2^2 + (3\omega^{-1/3}\mathrm{e}^{\omega/3} - I(\omega))^2]^2. \tag{4.9}$$

4.2. Application of boundary conditions

From $(4.1)_1$ and (2.38) we see that the appropriate boundary conditions are

$$\begin{aligned} &\Psi_0 = \mu_1, \quad \Psi_1 = \tfrac{1}{2}\tan\mu_1, \qquad \text{on} \quad \Theta = \alpha_1, \\ &\Psi_0 = -\mu_2, \ \Psi_1 = -\tfrac{1}{2}\tan\mu_2, \quad \text{on} \quad \Theta = \alpha_2, \end{aligned} \tag{4.10}$$

which are used to determine the values of the constants C_1 and C_2 in the leading-order solution Ψ_0 given by (4.4)–(4.5), and the constants C_3 and C_4 in the correction term Ψ_1 in $(4.8)_1$. The analysis for this procedure is given in Appendix D.

4.3. Results

In order to examine the accuracy and applicability of the full perturbation solution given by (4.1) of an axially symmetric hopper with a cone-in-cone insert, as depicted in Figure 3, we choose $\alpha_1 = \pi/6$ and $\alpha_2 = \pi/12$ ($\alpha_1 = 30^\circ$ and $\alpha_2 = 15^\circ$), noting from [5] that the angle that the sidewall of the hopper makes with the z-axis is generally assumed to be twice the angle that the insert makes with the z-axis. Further, we assume $\mu_1 = \mu_2 = \pi/12$, so that the surface on both sidewalls possess the same level of friction, and for four values of the angle of internal friction, namely $\phi = 7\pi/18,\ \pi/3,\ \pi/4$ and $\pi/6$, Figures 7, 8 and 9, respectively, show the comparison of $\Psi(\Theta)$, $G(\Theta)$ and $U(\Theta)/\bar{U}$ as determined from a full numerical solution of the governing Equations (2.30), (2.31) and (2.35), the zeroth-order approximation given by (4.4) and (4.6), and the full perturbation solution given by (4.1) and (4.8). We note that ψ is a

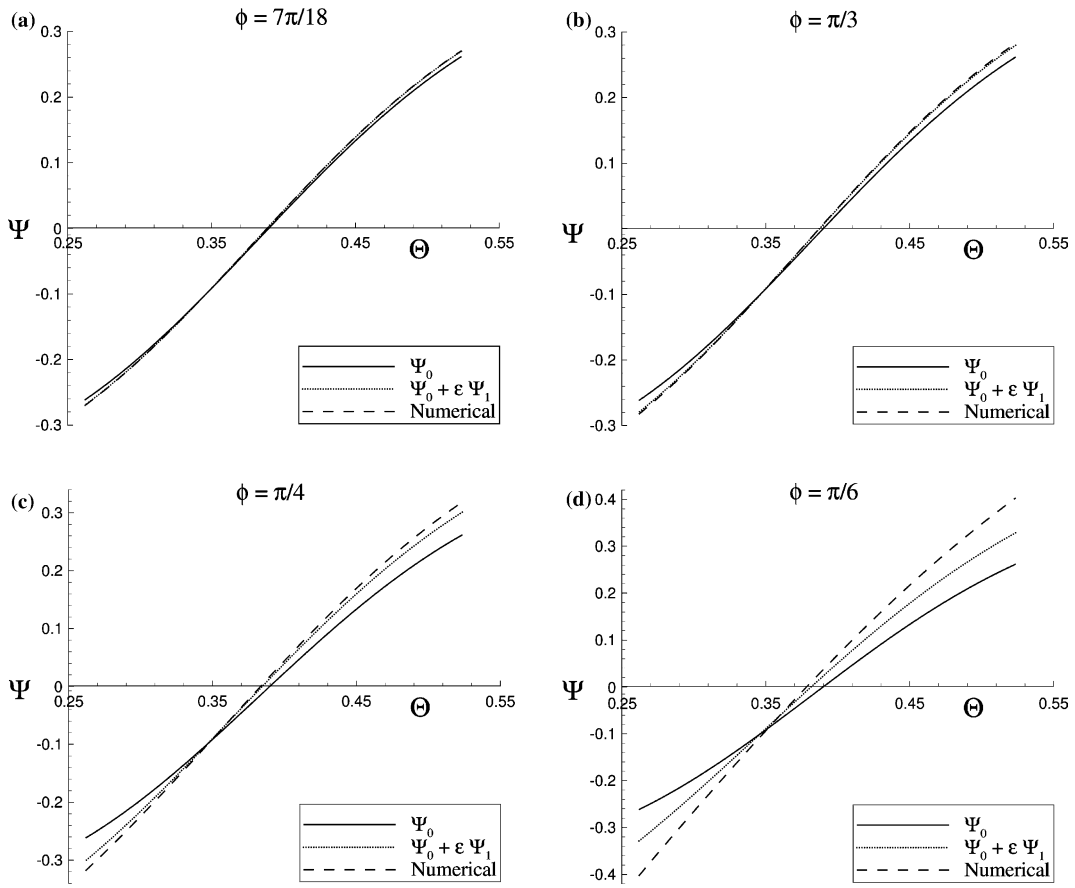

Figure 7. Comparison of the numerical, the zeroth-order and the full perturbation solutions for $\Psi(\Theta)$ for $\phi = 7\pi/18$, $\pi/3$, $\pi/4$ and $\pi/6$.

decreasing function of $\pi/2-\theta$ in Figure 4, while Ψ is an increasing function Θ in Figure 7. This behaviour arises since ψ is measured from the r-axis in the direction of increasing θ (not $\pi/2-\theta$), while Ψ is measured from the R-axis in the direction of increasing Θ. From Figure 9 we again find that near the middle of the material the magnitude of the velocity is greatest, while due to the material being "held up" on the walls, the velocity decreases towards both the insert and the hopper walls. Finally, due to gravity the material is again moving faster at the insert wall than the hopper wall.

From the figures, we see that the full perturbation solution gives an excellent estimate to the full numerical solution for values of angle of internal friction as low as $\phi = \pi/4$, while still providing a reasonable estimate for an angle of internal friction equal to $\phi = \pi/6$. For all cases considered, the full perturbation solution gives a much improved estimate than the zeroth-order solution, and we note that the steeper the sidewall of the hopper, the better the estimate from the full perturbation solution.

5. Rate of work

In this section we check the necessary physical condition of the rate of work being non-negative for both the two-dimensional and axially symmetric perturbation solutions presented in Sections 3 and 4, respectively.

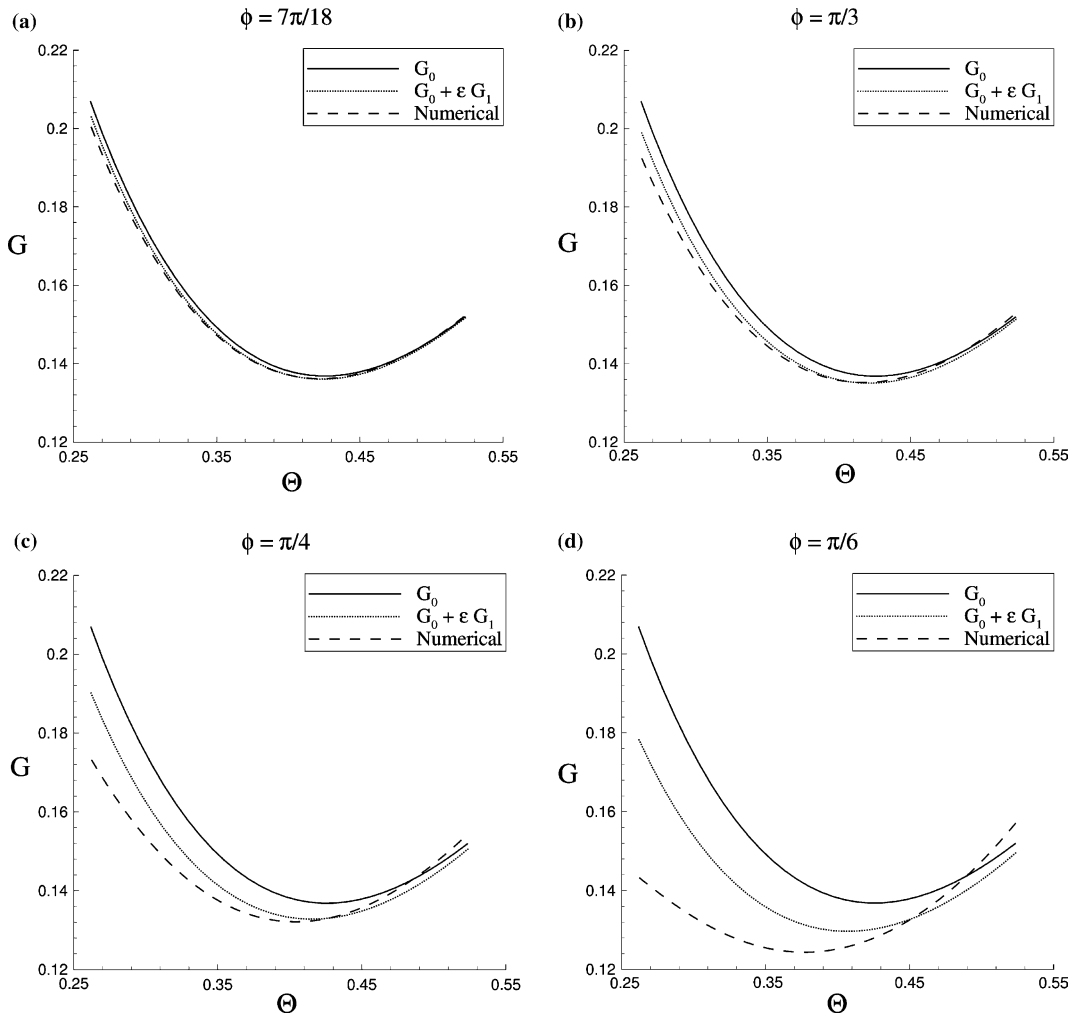

Figure 8. Comparison of the numerical, the zeroth-order and the full perturbation solutions for $G(\Theta)$ for $\phi = 7\pi/18,\ \pi/3,\ \pi/4$ and $\pi/6$.

5.1. Rate of work for the two-dimensional problem

To examine the rate of work for steady quasi-static plane strain gravity flow through a two-dimensional hopper with a wedge-in-wedge insert, we find from [37, page 482] that for the solution to be physical, the rate of plastic work is required to remain non-negative, resulting in the inequality

$$\frac{\mathrm{d}W}{\mathrm{d}t} = \mathrm{tr}(\boldsymbol{\sigma d}) \geq 0, \tag{5.11}$$

where $\mathrm{d}W/\mathrm{d}t$ denotes the rate of plastic work, tr denotes the usual trace of a tensor, $\boldsymbol{\sigma}$ is the Cauchy stress tensor and $\boldsymbol{d}$ is the strain-rate tensor. In terms of cylindrical polar coordinates (r, θ) for two-dimensional plane strain flow, as defined by Figure 2(b), the non-zero components of $\boldsymbol{\sigma}$ are σ_{rr}, $\sigma_{r\theta}$, $\sigma_{\theta\theta}$ and σ_{zz}, while the non-zero components of $\boldsymbol{d}$ are given by

$$d_{rr} = \frac{\partial v_r}{\partial r}, \quad d_{r\theta} = \frac{1}{2}\left[\frac{1}{r}\frac{\partial v_r}{\partial \theta} + \frac{\partial v_\theta}{\partial r} - \frac{v_\theta}{r}\right], \quad d_{\theta\theta} = \frac{1}{r}\frac{\partial v_\theta}{\partial \theta} + \frac{v_r}{r}. \tag{5.12}$$

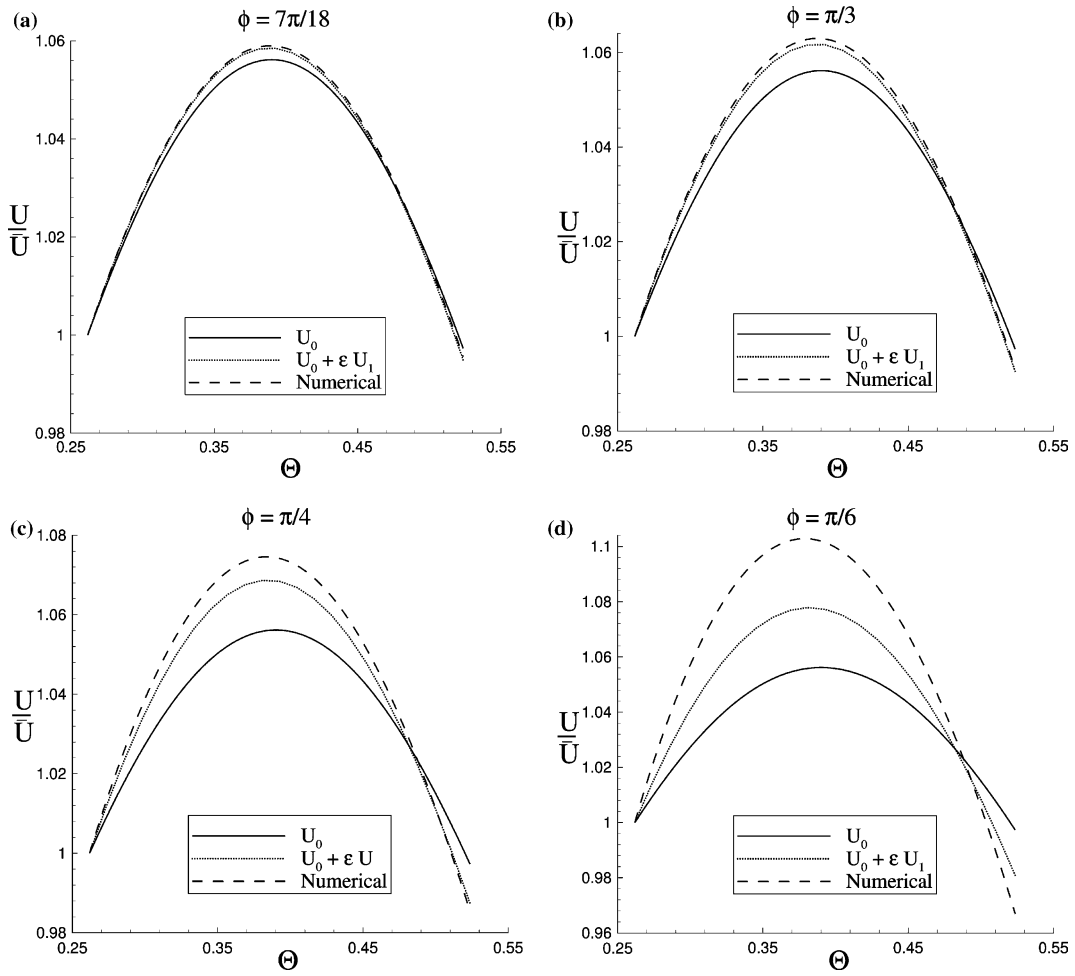

Figure 9. Comparison of the numerical, the zeroth-order and the full perturbation solutions for $U(\Theta)/\bar{U}$ for $\phi = 7\pi/18,\ \pi/3,\ \pi/4$ and $\pi/6$.

Thus, from (2.5), (5.11)–(5.12), we require

$$\begin{aligned}\frac{\mathrm{d}W}{\mathrm{d}t} &= \sigma_{rr}\frac{\partial v_r}{\partial r} + \sigma_{r\theta}\left[\frac{1}{r}\frac{\partial v_r}{\partial \theta} + \frac{\partial v_\theta}{\partial r} - \frac{v_\theta}{r}\right] + \sigma_{\theta\theta}\left[\frac{1}{r}\frac{\partial v_\theta}{\partial \theta} + \frac{v_r}{r}\right] \\ &= -p\left[\frac{\partial v_r}{\partial r} + \frac{1}{r}\frac{\partial v_\theta}{\partial \theta} + \frac{v_r}{r}\right] \\ &\quad + q\left\{\left[\frac{\partial v_r}{\partial r} - \frac{1}{r}\frac{\partial v_\theta}{\partial \theta} - \frac{v_r}{r}\right]\cos 2\psi + \left[\frac{\partial v_\theta}{\partial r} + \frac{1}{r}\frac{\partial v_r}{\partial \theta} - \frac{v_\theta}{r}\right]\sin 2\psi\right\} \geq 0, \end{aligned} \tag{5.13}$$

so that from $(2.14)_1$ and (2.16), the inequality (5.13) becomes

$$\sin 2\psi \frac{\mathrm{d}u}{\mathrm{d}\theta} - 2u\cos 2\psi \geq 0, \tag{5.14}$$

noting that $q \geq 0$. Further, from (2.17), (5.14) simplifies to give

$$\frac{1 + \sin\phi\cos 2\psi}{\sin\phi + \cos 2\psi} \geq 0,$$

since $u \leq 0$ (the flow of material is towards the apex of the hopper). We can immediately see that for the extreme case $\phi = \pi/2$ the rate of working is always positive. Given we have restricted ourselves to the range $-\pi \leq \psi \leq \pi$, for $\phi < \pi/2$ it follows that we must have

$$|\psi| < \frac{\pi}{4} + \frac{1}{2}\phi \tag{5.15}$$

for the rate of energy dissipation to remain non-negative.

For the two-dimensional problem considered in this paper, it is straightforward to test the rate of working condition (5.15). All that is required is to check the plots of ψ versus θ, like those presented in Figure 4. In fact, given the boundary conditions (2.20), we know that

$$\psi(\gamma_1) > -\left(\frac{\pi}{4} + \frac{1}{2}\phi\right), \quad \psi(\gamma_2) < \frac{\pi}{4} + \frac{1}{2}\phi,$$

so a sufficient condition for (5.15) to hold is that there are no local minima or maxima over the range $\gamma_1 < \theta < \gamma_2$. We have checked that the condition (5.15) holds true for a variety of parameter values, as required.

5.2. Rate of work for axially symmetric problem

For axially symmetric flow in terms of spherical polar coordinates (R, Θ, Φ) as defined by Figure 3, the non-zero components of $\boldsymbol{\sigma}$ are denoted by σ_{RR}, $\sigma_{R\Theta}$, $\sigma_{\Theta\Theta}$ and $\sigma_{\Phi\Phi}$ while the non-zero components of the rate-of-deformation tensor $\boldsymbol{d}$ are given by

$$d_{RR} = \frac{\partial V_R}{\partial R}, \quad d_{R\Theta} = \frac{1}{2}\left[\frac{1}{R}\frac{\partial V_R}{\partial \Theta} + \frac{\partial V_\Theta}{\partial R} - \frac{V_\Theta}{R}\right], \quad d_{\Theta\Theta} = \frac{1}{R}\frac{\partial V_\Theta}{\partial \Theta} + \frac{V_R}{R}, \quad d_{\Phi\Phi} = \frac{V_\Theta}{R}\cot\Theta + \frac{V_R}{R}.$$

Thus, from (2.21), (2.26) and (5.11), we require

$$\begin{aligned}\frac{\mathrm{d}W}{\mathrm{d}t} &= \sigma_{RR}\frac{\partial V_R}{\partial R} + \sigma_{R\Theta}\left[\frac{1}{R}\frac{\partial V_R}{\partial \Theta} + \frac{\partial V_\Theta}{\partial R} - \frac{V_\Theta}{R}\right] + \sigma_{\Theta\Theta}\left[\frac{1}{R}\frac{\partial V_\Theta}{\partial \Theta} + \frac{V_R}{R}\right] + \sigma_{\Phi\Phi}\left[\frac{V_\Theta}{R}\cot\Theta + \frac{V_R}{R}\right] \\ &= -P\left\{\frac{\partial V_R}{\partial R} + \frac{1}{R}\frac{\partial V_\Theta}{\partial \Theta} + \frac{2V_R}{R} + \frac{V_\Theta}{R}\cot\Theta\right\} + Q\left\{\left[\frac{\partial V_R}{\partial R} - \frac{1}{R}\frac{\partial V_\Theta}{\partial \Theta} - \frac{V_R}{R}\right]\cos 2\Psi + \right. \\ &\quad \left. + \left[\frac{1}{R}\frac{\partial V_R}{\partial \Theta} + \frac{\partial V_\Theta}{\partial R} - \frac{V_\Theta}{R}\right]\sin 2\Psi + \frac{V_\Theta}{R}\cot\Theta + \frac{V_R}{R}\right\} \geq 0,\end{aligned}$$

which, after substituting $(2.32)_1$ and (2.34), becomes

$$\sin 2\Psi \frac{\mathrm{d}U}{\mathrm{d}\Theta} + U(1 - 3\cos 2\Psi) \geq 0, \tag{5.16}$$

noting that $Q \geq 0$. Further, from (2.35), (5.16) simplifies to give the rate of work inequality

$$\frac{3 - \sin\phi + (3\sin\phi - 1)\cos 2\Psi}{\sin\phi + \cos 2\Psi} \geq 0. \tag{5.17}$$

We again note that for the special case of $\sin\phi = 1$, the rate of work inequality (5.17) is always satisfied. For all other values of ϕ, we must have

$$|\Psi| < \frac{\pi}{4} + \frac{1}{2}\phi. \tag{5.18}$$

This condition has been checked for a variety of parameter values for the problem considered in Section 4, and was found to hold true in each case. We conclude that the choice of hoop stress (2.26) is not inconsistent with the important requirement (5.11).

We mention that if the alternate condition (2.27) for the hoop stress was chosen, then (5.17) would be replaced with the similar condition

$$\frac{3+\sin\phi+(3\sin\phi+1)\cos 2\Psi}{\sin\phi+\cos 2\Psi}\geq 0.$$

However, this inequality also implies (5.18), so the necessary condition for non-negative energy dissipation would remain unchanged.

6. Conclusions

We have considered the problem of gravity flow of granular materials both in symmetrical hoppers with inserts and asymmetrical hoppers. These inserts are primarily used to influence the flow of the material to ensure that mass-flow occurs, rather than funnel-flow. For flow near the outlet of the hopper, we have applied the radial field stress similarity solutions, which give rise to highly non-linear coupled ordinary differential equations, while the flow fields have been determined using the non-dilatant double-shearing theory. We have analytically calculated the first two terms of a perturbation scheme valid for $1-\sin\phi\ll 1$, for both the stress and velocity fields, which are then applied to the problems considered. The perturbation results are in excellent agreement with a full numerical solution for large values of ϕ, as expected, and also gives reasonable predictions for values of ϕ as low as 45°.

We note here that the dynamic equations for Spencer's double-shearing theory are known to be linearly ill-posed (as are many other plasticity-type theories for granular flow), in the sense that small perturbations to existing solutions may grow exponentially in time (see [38], for example). This property puts some doubt on whether the steady solutions examined in this study actually describe real granular flows, although, as mentioned in the Introduction, there is experimental evidence (see [30], for example) that suggests the double-shearing theory is indeed appropriate for flows in the neighbourhood of a hopper outlet. This topic is still a matter for debate, and we have not pursued it here.

One of the goals of this study was to ascertain whether or not the perturbation solutions for highly frictional granular materials could be utilized for asymmetrical hoppers and symmetrical hoppers with inserts, in order to calculate the granular flow patterns near the outlet of the hopper. This has been achieved, and with the use of the non-dilatant double-shearing theory we have confirmed that the solutions presented satisfy the physically necessary requirement that the rate of working be non-negative. At present it is not precisely clear under what conditions an insert will convert a funnel-flow hopper into a mass-flow hopper (a simple idea involves the use of an envelope curve as discussed in Subsection 2.3) page 12, but with any future developments the results presented here may prove useful.

Appendix A. Correction terms in two-dimensions

Here we consider the ordinary differential Equation (3.9). With use of the change of variables (3.4), we can transform this equation into

$$(1+h^2)(h+\xi)\frac{\mathrm{d}^2\psi_1}{\mathrm{d}\xi^2}+2[1+h^2+2h(h+\xi)h']\frac{\mathrm{d}\psi_1}{\mathrm{d}\xi}+2\left[(h+\xi)h'^2-\frac{1+h^2}{h+\xi}h'\right]\psi_1$$
$$=h'^2\left[\frac{(1+\xi^2)^2}{(h+\xi)^2}-\xi(h+\xi)\right]+\frac{h(1+h^2)}{h+\xi}h',$$

which, after substituting the parametric solutions for h and ξ (3.6), can be transformed into

$$2\omega[C_2^2+I^2(\omega)]\frac{\mathrm{d}^2\psi_1}{\mathrm{d}\omega^2}+\left\{8\omega^{1/2}\mathrm{e}^{\omega/2}I(\omega)+(1-\omega)[C_2^2+I^2(\omega)]\right\}\frac{\mathrm{d}\psi_1}{\mathrm{d}\omega}+\{4\mathrm{e}^{\omega}+I^2(\omega)+C_2^2\}\psi_1$$
$$=-\frac{1}{2C_2}I(\omega)[C_2^2+I^2(\omega)]-\frac{2}{C_2}\mathrm{e}^{\omega}[2\omega^{-1/2}\mathrm{e}^{\omega/2}-I(\omega)]+\frac{1}{4C_2}\omega^{3/2}\mathrm{e}^{-\omega/2}[C_2^2+(2\omega^{-1/2}\mathrm{e}^{\omega/2}-I(\omega))^2]^2,$$

where ω is the parameter. Progress can be made by noting the left-hand side of this equation is simply

$$2\omega\frac{\mathrm{d}^2\Phi}{\mathrm{d}\omega^2}+(1-\omega)\frac{\mathrm{d}\Phi}{\mathrm{d}\omega}+\Phi,$$

where the variable Φ is defined by $\Phi=[C_2^2+I^2(\omega)]\psi_1$, so that we can integrate twice to find

$$\Phi=C_4(1-\omega)+\tfrac{1}{4}[2\omega^{1/2}\mathrm{e}^{\omega/2}+(1-\omega)I(\omega)]\left[\int_0^{\omega}(1-t)K(t)\mathrm{d}t+C_3\right]-$$
$$-\tfrac{1}{4}(1-\omega)\int_0^{\omega}[2t^{1/2}\mathrm{e}^{t/2}+(1-t)I(t)]K(t)\mathrm{d}t,$$

where C_3 and C_4 are constants and $K(t)$ is given by (3.11).

Now, by substituting the perturbation expansions $(3.1)_1$ and $(3.1)_2$ in (2.13), we find that

$$F_1=\frac{F_0}{2(1+\psi_0')}\{-2\psi_1'+2\psi_1(1+\psi_0')[\tan\psi_0+\cot(\theta+\psi_0)]+$$
$$+(1+\psi_0')\tan\psi_0[\tan\psi_0-\cot(\theta+\psi_0)]+\sec^2\psi_0\},$$

where F_0 is given by $(3.3)_1$. After making the transformations in (3.4), we arrive at the expression

$$F_1=\frac{F_0}{2(h+\xi)^2}\left\{2\frac{(1+h^2)(h+\xi)^2}{h'}\frac{\mathrm{d}\psi_1}{\mathrm{d}\xi}+2(1+h^2)(h+\xi)\psi_1+\right.$$
$$\left.+(1-h\xi)(1-2h\xi-h^2)-\frac{(1+h^2)^2}{h'}\right\},$$

which can be simplified further to $(3.10)_2$ with use of the parametric solutions (3.6).

Finally, from (2.18), $(3.1)_1$, $(3.1)_3$, (3.4) and (3.6) we find that u_1 is

$$u_1=u_0\int_{\theta}^{\theta_c}(2\psi_1+\tan\psi_0)\sec^2\psi_0\mathrm{d}\theta$$
$$=\frac{u_0}{8C_2^2}\left\{\mathrm{e}^{-\omega_c}[C_2^2+I^2(\omega_c)]^2-\mathrm{e}^{-\omega}[C_2^2+I^2(\omega)]^2+\right.$$
$$\left.+2\int_{\omega_c}^{\omega}t^{-1/2}\mathrm{e}^{-t/2}[C_2^2+I^2(t)][2C_2\psi_1+I(t)]\mathrm{d}t\right\},$$

where u_0 is the leading-order solution $(3.8)_2$, and ψ_1 is the correction term $(3.10)_1$. This expression may be simplified to give $(3.10)_3$.

Appendix B. General solution for asymmetrical wedge hopper

For an asymmetrical wedge hopper, the general solutions for the leading-order and correction terms in the region $\pi/2\le\theta\le\gamma_2$ are given here. The leading-order solution for ψ_0 is

$$\cot(\theta+\psi_0)=\frac{I(\omega)}{D_2},\quad \tan\theta=\frac{2s^{-1/2}\mathrm{e}^{s/2}-I(s)}{D_2},\tag{B.1}$$

where s acts as a parameter, $I(s) = J(s) + D_1$, and D_1 and D_2 are arbitrary constants. The solutions for F_0 and u_0 are given parametrically by

$$F_0 = \frac{1}{4}\frac{s^{-1/2}\mathrm{e}^{-s/2}[D_2^2 + I^2(s)]}{\left\{D_2^2 + [2s^{-1/2}\mathrm{e}^{s/2} - I(s)]^2\right\}^{1/2}}, \qquad u_0 = \frac{\bar{u}\, s\left\{D_2^2 + [2s^{-1/2}\mathrm{e}^{s/2} - I(s)]^2\right\}}{s_c\left\{D_2^2 + [2s_c^{-1/2}\mathrm{e}^{s_c/2} - I(s_c)]^2\right\}}, \tag{B.2}$$

where the parameter value $s = s_c$ corresponds to $\theta = \theta_c$. The correction terms are given by

$$\begin{aligned}
\psi_1 &= \frac{1}{D_2^2 + I^2(s)}\left\{D_4(1-s) + \frac{1}{4}[2s^{1/2}\mathrm{e}^{s/2} + (1-s)I(s)]\left[\int_0^s (1-t)K(t)\mathrm{d}t + D_3\right] - \right. \\
&\qquad \left. -\frac{1}{4}(1-s)\int_0^s [2t^{1/2}\mathrm{e}^{t/2} + (1-t)I(t)]K(t)\mathrm{d}t\right\}, \\
F_1 &= F_0\frac{s^{1/2}\mathrm{e}^{-s/2}}{8D_2^2}[D_2^2 + I^2(s)]\left\{8D_2\frac{\mathrm{d}\psi_1}{\mathrm{d}s} + 4D_2\psi_1 + (1+s)s^{-1/2}\mathrm{e}^{-s/2}[D_2^2 + I^2(s)]\right. \\
&\qquad \left. -6s^{-1/2}\mathrm{e}^{s/2}I(s) + \frac{8s^{-1}\mathrm{e}^s I^2(s)}{D_2^2 + I^2(s)}\right\}, \\
u_1 &= \frac{u_0}{8D_2^2}\left\{\mathrm{e}^{-s_c}[D_2^2 + I^2(s_c)]^2 - \mathrm{e}^{-s}[D_2^2 + I^2(s)]^2 + 2\int_{s_c}^s t^{-1/2}\mathrm{e}^{-t/2}[D_2^2 + I^2(t)][2D_2\psi_1 + I(t)]\mathrm{d}t\right\},
\end{aligned} \tag{B.3}$$

where D_3 and D_4 are constants of integration, F_0 given by $(\mathrm{B}.2)_1$, u_0 given by $(\mathrm{B}.2)_2$, and the function K given by the expression

$$\begin{aligned}
K(s) = &-\frac{1}{2D_2}s^{-1/2}\mathrm{e}^{-s/2}I(s)[D_2^2 + I^2(s)]^2 - \frac{2}{D_2}s^{-1/2}\mathrm{e}^{s/2}[2s^{-1/2}\mathrm{e}^{s/2} - I(s)] \\
&+ \frac{1}{4D_2}s\mathrm{e}^{-s}[D_2^2 + (2s^{-1/2}\mathrm{e}^{s/2} - I(s))^2]^2.
\end{aligned} \tag{B.4}$$

These expressions are equivalent to (3.6)–$(3.8)_2$ and $(3.10)_1$–(3.11), except we have assigned different labels to the parameter and the constants of integration.

Appendix C. Correction terms in axial symmetry

Here we consider the ordinary differential equation (4.7). With use of the change of variables (4.4), we can transform this equation into

$$\begin{aligned}
&(1+H^2)(\xi+H)\frac{\mathrm{d}^2\Psi_1}{\mathrm{d}\xi^2} + [4H(\xi+H)H' + 3(1+H^2)]\frac{\mathrm{d}\Psi_1}{\mathrm{d}\xi} + \left[2(\xi+H)H'^2 - \frac{3(1+H^2)}{\xi+H}H'\right]\Psi_1 \\
&\quad = \left[\xi(\xi+H) - \frac{(1+\xi^2)^2}{(\xi+H)^2}\right]H'^2 - \left[1 + (H-\xi)^2 - \frac{(1+\xi^2)^2}{(\xi+H)^2}\right]H' + \frac{(1+H^2)(H\xi-1)}{(\xi+H)^2},
\end{aligned}$$

which, after substituting the parametric solutions for H and ξ (4.4), can be transformed into

$$\begin{aligned}
&3\omega[C_2^2 + I^2(\omega)]\frac{\mathrm{d}^2\Psi_1}{\mathrm{d}\omega^2} + \{12\omega^{2/3}\mathrm{e}^{\omega/3}I(\omega) + (1-\omega)[C_2^2 + I^2(\omega)]\}\frac{\mathrm{d}\Psi_1}{\mathrm{d}\omega} + \{6\omega^{1/3}\mathrm{e}^{2\omega/3} + C_2^2 + I^2(\omega)\}\Psi_1 \\
&\quad = C_2\omega^{-1/3}\mathrm{e}^{\omega/3} + \frac{3}{C_2}\omega^{1/3}\mathrm{e}^{2\omega/3}[3\omega^{-1/3}\mathrm{e}^{\omega/3} - I(\omega)] - \frac{1}{9C_2}\omega^{1/3}\mathrm{e}^{-\omega/3}(1+\omega)[C_2^2 + (3\omega^{-1/3}\mathrm{e}^{\omega/3} - I(\omega))^2]^2 + \\
&\qquad + \frac{1}{C_2}\omega^{-1/3}\mathrm{e}^{\omega/3}[2I(\omega) - 3\omega^{-1/3}\mathrm{e}^{\omega/3}]^2 + \frac{1}{9C_2}\omega^{-2/3}\mathrm{e}^{-\omega/3}[C_2^2 + I^2(\omega)][3\omega^{-1/3}\mathrm{e}^{\omega/3}I(\omega) - C_2^2 - I^2(\omega)],
\end{aligned}$$

where ω is the parameter. Progress can be made by noting that the left-hand side of this equation is simply

$$3\omega\frac{\mathrm{d}^2\Phi}{\mathrm{d}\omega^2}+(1-\omega)\frac{\mathrm{d}\Phi}{\mathrm{d}\omega}+\Phi,$$

where the variable Φ is defined to be $\Phi=[C_2^2+I^2(\omega)]\Psi_1$, so that we can integrate twice to find

$$\Phi=C_4(1-\omega)+\frac{1}{9}[3\omega^{2/3}\mathrm{e}^{\omega/3}+(1-\omega)I(\omega)]\left[\int_0^{\omega}(1-t)K(t)\mathrm{d}t+C_3\right]$$
$$-\frac{1}{9}(1-\omega)\int_0^{\omega}[3t^{2/3}\mathrm{e}^{t/3}+(1-t)I(t)]K(t)\mathrm{d}t,$$

where C_3 and C_4 are constants and $K(t)$ is given by (4.9).

Now, by substituting the perturbation expansions $(4.1)_1$ and $(4.1)_2$ in (2.31), we find that

$$G_1=-\frac{G_0}{2}\left\{\frac{2\Psi_1'+\cot\Theta\tan\Psi_0-2\tan^2\Psi_0-1}{1+\Psi_0'}+2\Psi_1[\tan(\Theta+\Psi_0)-\tan\Psi_0]\right.$$
$$\left.-\tan\Psi_0[\tan(\Theta+\Psi_0)+\tan\Psi_0]\right\},$$

where G_0 is given by $(4.3)_1$, and can be simplified to $(4.8)_2$ with the use of the parametric solutions (4.4).

Finally, from (2.36), $(4.1)_1$, $(4.1)_3$ and (4.4), we find that U_1 is

$$U_1=-\frac{3U_0}{2}\int_{\Theta_c}^{\Theta}(2\Psi_1+\tan\Psi_0)\sec^2\Psi_0\ \mathrm{d}\Theta,$$
$$=-\frac{U_0}{6C_2^2}\int_{\omega_c}^{\omega}t^{-2/3}\mathrm{e}^{-t/3}[C_2^2+I^2(t)][2C_2\Psi_1+I(t)]\mathrm{d}t+\frac{U_0}{18C_2^2}\int_{\omega_c}^{\omega}t^{-1/3}\mathrm{e}^{-2t/3}[C_2^2+I^2(t)]^2\mathrm{d}t,$$

where U_0 is the leading-order solution $(4.6)_2$, and Ψ_1 is the correction term $(4.8)_1$. This expression may be simplified to give $(4.8)_3$.

Appendix D. Constants of integration for axial symmetry

In the following, we will use the integral

$$J(\omega)=\int_0^{\omega}t^{-1/3}\mathrm{e}^{t/3}\mathrm{d}t, \tag{D.1}$$

so that from (4.5) we have $I(\omega)=J(\omega)+C_1$. Now, for the case of a cone-in-cone insert (see Figure 3) we need only consider the domain $\alpha_2\le\Theta\le\alpha_1$, since the flow is symmetrical around $\Theta=0$. We suppose that the parameter ω in (4.4) takes the values $\omega=\omega_1$ and $\omega=\omega_2$ at $\Theta=\Theta_1$ and $\Theta=\Theta_2$, respectively. By applying the boundary conditions $(4.10)_1$ and $(4.10)_3$, we find the constants C_1 and C_2 are given in terms of these parameter values by

$$C_1=C_2\tan(\alpha_1+\mu_1)-J(\omega_1),\ C_2=\frac{3\omega_2^{-1/3}\mathrm{e}^{\omega_2/3}-J(\omega_2)+J(\omega_1)}{\cot\alpha_2+\tan(\alpha_1+\mu_1)}, \tag{D.2}$$

while the values of ω_1 and ω_2 are determined by the pair of transcendental equations

$$\frac{1}{3}\omega_2^{1/3}\mathrm{e}^{-\omega_2/3}[J(\omega_1)-J(\omega_2)]=\frac{\tan(\alpha_1+\mu_1)-\tan(\alpha_2-\mu_2)}{\cot\alpha_2+\tan(\alpha_2-\mu_2)},$$
$$\left(\frac{\omega_2}{\omega_1}\right)^{1/3}\mathrm{e}^{(\omega_1-\omega_2)/3}=\frac{\cot\alpha_1+\tan(\alpha_1+\mu_1)}{\cot\alpha_2+\tan(\alpha_2-\mu_2)}.$$

The other two boundary conditions $(4.10)_2$ and $(4.10)_4$ provide the following equations for C_3 and C_4

$$C_3 = \frac{1}{M(\omega_1) - mM(\omega_2)} \left\{ \frac{9}{2}(m \tan \mu_2 [C_2^2 + I^2(\omega_2)] + \tan \mu_1 [C_2^2 + I^2(\omega_1)]) + \right.$$
$$\left. + (1-\omega_1) \int_{\omega_2}^{\omega_1} M(t)K(t)\mathrm{d}t + mM(\omega_2) \int_0^{\omega_2} (1-t)K(t)\mathrm{d}t - M(\omega_1) \int_0^{\omega_1} (1-t)K(t)\mathrm{d}t \right\},$$
$$C_4 = \frac{1}{M(\omega_1) - mM(\omega_2)} \left\{ -\frac{1}{2(1-\omega_2)} (\tan \mu_1 M(\omega_2)[C_2^2 + I^2(\omega_1)] + \tan \mu_2 M(\omega_1)[C_2^2 + I^2(\omega_2)]) + \right.$$
$$\left. + \frac{M(\omega_1)M(\omega_2)}{9(1-\omega_2)} \int_{\omega_2}^{\omega_1} (1-t)K(t)\mathrm{d}t - \frac{1}{9} \left[mM(\omega_2) \int_0^{\omega_1} M(t)K(t)\mathrm{d}t - M(\omega_1) \int_0^{\omega_2} M(t)K(t)\mathrm{d}t \right] \right\},$$

where $M(\omega)$ and m are defined by

$$M(\omega) = 3\omega^{2/3} \mathrm{e}^{\omega/3} + (1-\omega)I(\omega), \qquad m = \frac{1-\omega_1}{1-\omega_2},$$

respectively.

Acknowledgements

This work is supported by the Australian Research Council through an Australian Post-Doctoral Fellowship (GMC), a Discovery Project Grant (SWM) and an Australian Professorial Fellowship (JMH). NT gratefully acknowledges the Institute for the Promotion of Teaching Science and Technology, Thailand, for financial support. The authors are also grateful to one of the referees for a number of helpful comments, and in particular for recommending that the authors confirm the physical applicability of the solutions presented here by establishing the non-negative rate of working as described in Section 5.

References

1. A. Drescher, *Analytical Methods in Bin-load Analysis*. Amsterdam: Elsevier (1991) 255pp.
2. J.M. Hill and G.M. Cox, Cylindrical cavities and classical rat-hole theory occuring in bulk materials. *Int. J. Num. Anal. Meth. Geomech.* 24 (2000) 971–990.
3. J.M. Hill and G.M. Cox, Stress profiles for tapered cylindrical cavities in granular media. *Int. J. Solids Struct.* 38 (2001) 3795–3811.
4. A.J.M. Spencer and J.M. Hill, Non-dilatant double-shearing theory applied to granular funnel-flow in hoppers. *J. Engng. Maths.* 41 (2001) 55–73.
5. J.R. Johanson, Controlling flow patterns in bins by use of an insert. *Bulk Solids Handling* 2 (1982) 495–498.
6. J.R. Johanson and W.K. Kleysteuber, Flow-corrective inserts in bins. *Chem. Engng. Progr.* 62 (1966) 79–83.
7. U. Tüzün and R.M. Nedderman, Gravity flow of granular materials round obstacles – I. Investigation of the effects of inserts on flow patterns inside a silo. *Chem. Engng. Sci.* 40 (1985) 325–336.
8. U. Tüzün and R.M. Nedderman, Gravity flow of granular materials round obstacles – II. Investigation of the stress profiles at the wall of a silo with inserts. *Chem. Engng. Sci.* 40 (1985) 337–351.
9. S. Ding, S.R. De Silva and G.G. Enstad, Effect of passive inserts on the granular flow from silos using numerical solutions. *Particulate Sci. Tech.* 21 (2003) 211–226.
10. S-C. Yang, S-S. Hsiau, The simulation and experimental study of granular materials discharged from a silo with the placement of inserts. *Powder Technol.* 120 (2001) 244–255.
11. B. Dantoin, R. Hossfeld and K. McAtee, Converting from funnel-flow to mass-flow. *Power* 147 (2003) 61.
12. A.W. Roberts, Bulk solids handling: Recent developments and future directions. *Bulk Solids Handling* 11 (1991) 17–35.
13. P.A. Gremaud and J.V. Matthews, On the computation of steady hopper flows I. Stress determination for Coulomb materials. *J. Comp. Phys.* 166 (2001) 63–83.

14. P.A. Gremaud, J.V. Matthews and D.G. Schaeffer, Secondary circulation in granular flow through nonaxisymmetric hoppers. *SIAM J. Appl. Math.* 64 (2003) 583–600.
15. A.W. Jenike, Steady gravity flow of frictional-cohesive solids in converging channels. *J. Appl. Mech.* 31 (1964) 5–11.
16. A.W. Jenike, Gravity flow of frictional-cohesive solids - Convergence to radial stress fields. *J. Appl. Mech.* 32 (1965) 205–207.
17. J.R. Johanson, Stress and velocity fields in the gravity flow of bulk solids. *J. Appl. Mech.* 31 (1964) 499–506.
18. V.V. Sokolovskii, *Statics of Granular Media*. Oxford: Pergamon Press (1965) 270pp.
19. G.M. Cox and J.M. Hill, Some exact mathematical solutions for granular stock piles and granular flow in hoppers. *Math. Mech. Solids* 8 (2003) 21–50.
20. J.M. Hill and G.M. Cox, An exact parametric solution for granular flow in a converging hopper. *Z. Angew Math. Phys. (ZAMP)* 52 (2001) 657–668.
21. N. Thamwattana and J.M. Hill, Perturbation solutions for highly frictional granular media. *Proc. R. Soc. London A* 461 (2005) 21–42.
22. Australian Standards, *Loads on Bulk Solids Containers*. Australian Standards 3774 (1996) 77pp.
23. S.W. Perkins, Non-linear limit analysis for the bearing capacity of highly frictional soils. In: J.P. Mohsen (ed), *Proc. 2nd Congress on Computing in Civil Engineering, Atlanta*, 4 June 1995, ASCE (1995) pp. 629–636.
24. S.W. Perkins, Bearing capacity of highly frictional material. *ASTM Geotech. Testing J.* 18 (1995) 450–462.
25. S. Sture, Constitutive issues in soil liquefaction. In: P.V. Lade and J.A. Yanamuro (eds.), *Proc. Physics and Mechanics of Soil Liquefaction, Baltimore*, 10–11 September 1998, Balkema (1999) pp. 133–143.
26. A.J.M. Spencer, A theory of the kinematics of ideal soils under plane strain conditions. *J. Mech. Phys. Solids* 21 (1964) 337–351.
27. A.J.M. Spencer, Deformation of ideal granular materials. In: H.G. Hopkins and M.J. Sewell (eds.), *Mechanics of Solids: The Rodney Hill 60th Anniversary Volume*. Oxford: Pergamon (1982) pp. 607–652.
28. A.J.M. Spencer, Remarks on coaxiality in fully developed gravity flows of dry granular materials. In: N.A. Fleck and A.C.F. Cocks (eds.), *Mechanics of Granular and Porous Materials*. Dordrecht: Kluwer Academic Publishers (1997) pp. 227–238.
29. A.J.M. Spencer and N.J. Bradley, Gravity flow of a granular material in compression between vertical walls and through a tapering vertical channel. *Q. J. Mech. Appl. Math.* 45 (1992) 733–746.
30. P.A. Gremaud, Numerical issues in plasticity models for granular materials. *J. Volcanol. Geotherm. Res.* 137 (2004) 1–9.
31. G.M. Cox and J.M. Hill, Some exact velocity profiles for granular flow in converging hoppers, *Z. Angew Math. Phys. (ZAMP)* 56 (2005) pp. 92–106.
32. S.W. McCue and J.M. Hill, Free surface problems for static Coulomb–Mohr granular solids. *Mathematics and Mechanics of Solids* (2005) to appear.
33. A.D. Cox, G. Eason and H.G. Hopkins, Axially symmetric plastic deformations in soils. *Phil. Trans. R. Soc. London A* A254 (1961) 1–45.
34. A.J.M. Spencer and N.J. Bradley, Gravity flow of granular materials in converging wedges and cones. In: K.Z. Markov (ed.), *Proc. 8th Int. Symp. Continuum Models and Discrete Systems, Varna, Bulgaria*, 11–16 June 1995, Singapore: World Scientific (1996) pp. 581–590.
35. S.W. McCue, I.K. Johnpillai and J.M. Hill, New stress and velocity fields for highly frictional granular materials. *IMA J. Appl. Math.* 70 (2005) pp. 92–118.
36. R.L. Burden and J.D. Faires, *Numerical Analysis*. Boston: PWS Publishing (1993) 841pp.
37. S.C. Hunter, *Mechanics of Continuous Media*. Chichester: Ellis Horwood Limited (1983) 640pp.
38. D. Harris, Ill- and well-posed models of granular flow. *Acta Mech.* 146 (2001) 199–225.